Pfeiffer, M., Aburto, F., Le Roux, J. P., Kemnitz, H., Sedov, S., Solleiro-Rebolledo, E., Seguel, O. (2012): Development of a Pleistocene calcrete over a sequence of marine terraces at Tongoy (north-central Chile) and its paleoenvironmental implications. - Catena, 97, 104-118

DOI: 10.1016/j.catena.2012.05.008

Development of a Pleistocene calcrete over a sequence of marine terraces at Tongoy (north-central Chile) and its palaeoenvironmental implications

Marco Pfeiffer [1, 2,*], Felipe Aburto [3,2], Jacobus P. Le Roux[1], Helga Kemnitz[4], Sergey Sedov[5], Elizabeth Solleiro-Rebolledo[5], Oscar Seguel[2]

1. Departamento de Geología, Facultad de Ciencias Físicas y Matemáticas, Universidad de Chile / Centro de Excelencia en Geotermia Andina, Plaza Ercilla 803, 8370450 Santiago, Chile

2. Departamento de Ingeniería y Suelos, Facultad de Ciencias Agronómicas, Universidad de Chile, Santa Rosa 11315, 8820808 La Pintana, Chile

3. Soils and Biogeochemistry Graduate Group, University of California Davis, USA

4. Helmholtz Center, Deutsches GeoForschungsZentrum, Section 3.1, Telegrafenberg, 14473, Germany

5. Instituto de Geología, Universidad Nacional Autónoma de México, Del. Coyoacán 04510 D.F. México

*Corresponding autor: Departamento de Ingeniería y Suelos, Facultad de Ciencias Agronómicas, Universidad de Chile, Santa Rosa 11315, 8820808 La Pintana, Chile. Tel.: +56-2-9785735; Fax: +56-2-9785746

E-mail addresses: mpfeiffer@ug.uchile.cl, feaburto@ucdavis.edu, jroux@cec.uchile.cl, heke@gfz-potsdam.de, sergey@geologia.unam.mx, solleiro@geologia.unam.mx, oseguel@uchile.cl

Abstract

The importance of the Norte Chico region in north-central Chile has long been recognized for the paleoclimates recorded in its soils. This area lies in an extreme climate gradient between the hyper-arid Atacama Desert in the north and a Mediterranean climate in the south, which has made it very sensitive to past climate changes. Nevertheless, few paleoclimate studies have been undertaken in the region, and these were mostly concentrated on the Holocene. We studied Pleistocene climate changes recorded in soils that formed over a series of marine terraces near Tongoy about 60 km south of La Serena. The calcrete and soil development took place on four marine terraces associated with Marine Isotope Stages MIS 11, MIS 7e, MIS 5e, and MIS 1. The different types of calcretes that developed on the three oldest terraces containing calcareous material indicate that they developed during different periods, and that climatic conditions favorable for the development of these soils existed in the area at least from MIS 11 (412 ka) until post-MIS 5e (125 ka). The calcrete horizons show well-defined development stages recording cyclic climate changes varying between arid and more humid during the late Pleistocene. These climate changes recorded in the Tongoy soils are reflected by sedimentological, geomorphological and pedogenic processes. Climate cycles have only been recorded previously for the post-MIS 5e stage in the area, this study being the first to include climate variations reaching MIS 11.

1. Introduction

The Norte Chico region in north-central Chile lies in a transition zone between the hyper-arid Atacama Desert to the north and the Mediterranean climate of central Chile to the south, which makes this region sensitive to Quaternary climate changes (Miller, 1976). However, paleoclimate studies in this region have concentrated mainly on the Holocene, with very little data on the Pleistocene (Grosjean et al., 1997, 1998; Lamy et al., 1998, 2000; Maldonado and Villagrán, 2002, 2006; Veit, 1996; Villagrán and Varela, 1990). Up to now, paleoclimate studies of the area have only gone back to approximately 120,000 yr BP (Lamy et al., 1998). Despite controversies about the exact timing and duration of paleoclimate changes in the region, all published records show an alternation of wet and dry periods (Latorre et al., 2007). These are associated with latitudinal shifts of the climate zones along the South American Pacific margin linked to north–south displacements of the Southern Westerlies (Lamy et al.,

2000). Soils with carbonate accumulation are common in Mediterranean semi-arid regions (Yaalon, 1997) and are characterized by calcium carbonates that are known to be important paleoenvironmental proxies (Cerling and Quade, 1993; Durand et al., 2010; Gocke et al., 2011; Tanner, 2010). Such soils commonly develop into calcretes forming sub-profiles within the main soil profiles (Wright and Tucker, 1991). Despite the recognition by several authors of "relict" pedogenic features in the soils of Norte Chico (Casanova et al., 2010; Franz, 1966; Fuenzalida, 1951; Paskoff, 1970; Wright and Espinoza, 1962), only one study combined a pedological interpretation with absolute dating in a paleoclimatic reconstruction of the area (Veit, 1996). However, there are so far no paleoclimatic studies that are based on pedogenic carbonates in the Norte Chico region, even though such studies have been carried out successfully in the Atacama Desert by Berger and Cooke (1997), Latorre et al. (1997), Rech et al. (2003), and Quade et al. (2007). The objective of this study is to reconstruct the sequence of events in the development of the Tongoy soil profiles, to which end we examined 20 profiles distributed over four marine terraces, of which seven have been analyzed in detail. This paper presents the complex geomorphological and paleoclimatic history of the Tongoy soils, in an area of great interest to paleoclimatologists, geomorphologists and pedologists.

2. Regional setting and soil forming factors

The study area is located on the north-central Pacific Coast of Chile (Fig. 1) within the area formerly occupied by the Tongoy paleobay (Le Roux et al., 2006). This depression forms part of a Cenozoic basin filled with marine deposits of Mio-Pleistocene age that are known as the Coquimbo Formation (Le Roux et al., 2006). The bayfill deposits include mudstones, sandstones, coquinas and conglomerates that accumulated during a series of transgressions and regressions related to tectonic movements combined with global sea level variations, studied in detail by Olivares (2004) and Le Roux et al. (2006). Variation of the relative sea level combined with continental uplift generated a series of wave-cut marine terraces since the middle Pleistocene in the area, which have been studied by several authors (Benado, 2000; Brüggen, 1950; Chávez, 1967; Darwin, 1846; Domeyko, 1848; Heinze, 2003; Herm, 1969; Ota et al., 1995; Paskoff, 1970; Pfeiffer, 2011; Radtke, 1989; Saillard, 2008). Ota et al. (1995) identified four marine terraces in the area of Altos de Talinay and three terraces in the Tongoy paleobay, which they designated TII, TIII and TIV in order of decreasing age. The TI terrace only appears in the Altos de Talinay area, so that the TII terrace is the oldest for the Tongoy area (Fig. 1). Radtke (1989) made an unsuccessful attempt to determine the chronology of the four terraces at Tongoy by Electron Spin Resonance (ESR) and U/Th disequilibria on marine shells, obtaining a wide range of ages for similar geological and topographic conditions, which he explained as being a result of deposit mixing during the different marine transgressions that reoccupied the same terrace. This conclusion was also reached by Hsu et al. (1989). However, at the Bay of Coquimbo north of the present study area, Radtke (1989) successfully dated marine terraces using U-series on marine shells. These data were used by Ota et al. (1995) to assign ages to the Tongoy terraces based on geomorphological correlation with the Coquimbo Bay terraces, which are almost continuous with those at Tongoy. According to this study, the relative ages of the terraces are Plio-Pleistocene for TI, middle Pleistocene for TII, MIS 9 for TIII and MIS 5e for TIV. The Holocene level was later assigned to TV by Benado (2000), incorporating the present beach as a terrace level, which was previously studied and dated by Ota and Paskoff (1993). The latter authors recognized a series of beach ridges that correspond to a Holocene marine regression episode, in which the oldest beach ridge has a 14C age of 5400 yrs BP and the youngest a 14C age of 910 yrs BP. Saillard (2008) undertook U–Th dating on marine shells of the TII and TIV terraces and assigned them to MIS 11 and MIS 5e, respectively. The TIV terrace age of Saillard (2008) coincides with ages proposed by Ota et al. (1995) and Benado (2000). The TII terrace age poses some questions: many authors agree that there is a geomorphological correlation

between the Tongoy and Altos de Talinay terraces, the latter having been dated by Saillard et al. (2009) using 10Be, based on which the TII level was assigned to MIS 9. Regard et al. (2010) proposed that this terrace, extending almost continuously between 15°S and 30°S, formed due to repeated superimposed highstands during a prolonged period of uplift, in which the latest marine transgression corresponds to MIS 11. Terrace TIII is assumed to be of the same age in the Tongoy and Talinay areas according to geomorphological correlation (Table 1), having been dated and assigned to MIS 7e by Saillard et al. (2009). The gap from MIS 11 to MIS 7 existing between the TII and TIII terraces at Tongoy, could be explained by slow uplift after MIS 9 that reoccupied the MIS 9 level during MIS 7 in the Tongoy area. A similar process was described by Saillard et al. (2009) for the Talinay area. In this study we used the terrace ages proposed by the authors mentioned in Table 1.

The soil profiles show two parent materials that are clearly separated by a discontinuity: a marine substrate and an overlying eolian sand, (Herm, 1969; Paskoff, 1970; Pfeiffer et al., 2011). The marine deposit is composed of (i) coarse, sandy Balanus coquina of the Coquimbo Formation, as for example in the Almendros profile (Olivares, 2004), (ii) clay and silt corresponding to deep bayfill deposits of the Coquimbo Formation described by Olivares (2004) and Le Roux et al. (2006), as in the Las Lomas profile, or (iii) deposits corresponding to marine regression after the sea level highstands of MIS 11 (Maitencillo, La Montosa and Alamito profiles), MIS 5e (El Rincón profile), or the Holocene regression reflected in the younger beach profile (Ota and Paskoff, 1993). In all profiles, the surface eolian deposit evolved into a sandy soil of 15 to 60 cm depth. The present climate of Tongoy is semi-arid Mediterranean with precipitation concentrated in winter and a moisture deficit for at least 9 months per year. The mean annual precipitation for the locality is 85 mm with an evapo-transpiration potential of 351 mm. The mean annual temperature is 13.6 °C, with a mean annual minimum of 9.2 °C, and a mean annual maximum of 20.6 °C (CIREN, 1990). The older soils have passed through different climate periods, with large-scale variations related to glacial cycles. The latter were characterized by more humid periods during glacial stages due to the latitudinal shift of the Southern Westerlies (Lamy et al., 1998, 2000). Smaller-scale climate variations alternated between arid and moist during the Holocene (Grosjean et al., 1997, 1998; Maldonado and Villagrán, 2002, 2006; Veit, 1996). The natural vegetation is composed of steppe forest (Gajardo, 1994), with a few tree species such as Acacia caven, Porlieria chilensis and Lithraea caustica, and lowshrubs including Baccharis paniculata, Ephedra chilensis, Flourensia thurifera, and Bahia ambrosioides, among others. Cactus species include Eulychnia breviflora, Cumulopuntia sphaerica, Eryosyce sp. and Echinopsis chiloensis, whereas herbaceous species are mainly of annual growth habit. About 30 km south of the study area lies the Fray Jorge National Park, which corresponds to a temperate humid forest in the Altos de Talinay area. Its existence is interpreted as a relict of Miocene age when the climate was more humid than at present (Villagrán et al., 2004). The study area has been subjected to intensive agricultural activities over the past decades and the introduction of the shrub Atriplex nummularia, which is used as forage for sheep and goat farming in the area (Cuevas and Vega, 2006).

3. Methodology

We examined more than 20 soil profiles in trenches, road cuts and open pit mines, from which seven profiles were selected for detailed field description and laboratory analysis. The selected soil profile locations are shown in Fig. 2, and their ages were assumed to be the age of the marine terraces on which they developed (Table 1). However, due to the great extent of the TII terrace, we estimated approximate ages for the soil profiles according to the chronology of marine retreat after MIS 11 proposed by Sidall et al. (2006) and the distance

to the inner border of the TII terrace, as shown in Fig. 3. For this estimation we considered that impacting waves at Tongoy met the conditions for low cliff erosion of the terraces as described by Anderson et al. (1999) for shallow marine shelves. Since the topography, bathymetry and wave dynamics at Tongoy cause wave energy dissipation that does not generate significant coastal erosion (Moraga and Olivares, 1993; Villagrán, 2007) we assumed the NW border of terrace TII to have been close to the maximum marine regression (Fig. 3). Soils were described according to the methodology proposed by Schoenberger et al. (2002) and calcrete soil profiles were classified following the Machette (1985) sequence of calcrete development. Soil samples were taken from each genetic horizon for chemical, physical, mineralogical and micromorphological analysis, those from the TII terrace being the same as those used in a previous study (Pfeiffer et al., 2011). Particle size distribution was determined by sieve and pipette analysis according to Bouyoucos (1936), after the removal of carbonates with HCl, the destruction of organic matter, and dispersion with sodium pyrophosphate. Bulk density was measured by the clod method, whereas excavation methods were used for surficial horizons (Grossman and Reinchs, 2002). In order to classify the soil, standard methods were applied in determining their properties as recommended for Chilean soils by Sadzawka et al. (2004). Soil samples were analyzed at the Laboratory of Soil and Water Chemistry of the Soil Sciences Department at the Universidad de Chile. Electrical conductivity (EC) of the saturation extract was measured with a CON 510 Oakton bench conductivity meter. Soil reaction (pH) was measured in water (1:2.5) with a Corning model 7 pH meter. Soil organic carbon content was determined according to the Walkley-Black method and a standard conversion factor of 1.724 was used to convert Walkley-Black carbon into organic matter (OM) content. Soil extractable cations (Na^+, K^+, Ca^{2+}, Mg^{2+}) were extracted by ammonium acetate solution at a pH of 7.0 and the Ca and Mg contents were determined by atomic absorption spectroscopy using a Perkin Elmer 3110 atomic absorption spectrometer. K and Na were determined by flame photometry using Jenway PFP 7 equipment. Similarly, the Cation Exchange Capacity (CEC) was estimated by measuring soil-extractable Na after NaOAc saturation using the same equipment. Thin sections were prepared from undisturbed soil samples impregnated with resin, and studied under a petrographic microscope. The descriptions of soil thin sections were made following Bullock et al. (1985), Wright and Tucker (1991), and Stoops (2003). The soils where classified according to the Soil Taxonomy (Soil Survey Staff, 2010) and World Reference Base for Soil Resources (WRB) (IUSS Working Group WRB, 2006). Quartz grain surface analysis for terrace TII profiles used in a previous study (Pfeiffer et al., 2011) are also presented, in addition to new data from the Las Lomas profile (TIV), for which the same methodology as in Pfeiffer et al. (2011) was used. In total, four profiles were used for quartz grain surface analysis.

The clay mineralogy of 22 selected soil horizons was analyzed using X-ray diffraction (XRD), based on the methodology described by Jackson (1975). The organic matter of previously sieved samples (b0.0038 mm), was removed using an adjusted pH of 9.5 in a sodium hypochlorite solution (5.25 wt.%). Clay was later separated by centrifugation as described by the same author. Two subsamples of each clay suspension were washed with HCl (pH 3.5). One of these samples was K-saturated using a 1 M KCl solution (hereafter referred to as KCl treatment), while the other was saturated using 1 M $MgCl_2$ (MgCl treatment). XRD patterns of the oriented aggregate specimens were obtained using a Rigaku model Ultima IV X/ray diffractometer with a Cu Kα1 target operating at 40 V and 40 mA. Subsequently, the KCl treated samples were heated for 2 h, first at 350 °C (350 treatment) and subsequently at 550 °C. The Mg saturated samples were then solvated with glycerol (glycerol treatment) in order to differentiate between vermiculite, chlorite and smectitic species (Whittig and Allardice, 1986). A semi-quantitative comparison of diffraction maxima at 1.42 nm (d-spacing) after different treatments was used to discriminate between vermiculite,

chlorite and poorly crystalline smectites. Diffraction maxima at 0.720 nm and 0.445 nm after KCl treatment and disappearance after heating were used to determine the presence of kaolinite. The presence of micas was determined using diffraction maxima at 1.01–0.99 nm and 0.33. In order to differentiate between trioctahedral and dioctahedral micas we performed low speed powder diffraction XRD analysis of selected samples with angles between 59.0 and 62.02. We used a low intensity peak at 0.150 nm to determine the presence of muscovite (Fanning et al., 1989). Additionally, selected representative samples were subjected to differential scanning calorimetry (DSC) to detect the presence of smectites (dehydration between 25 and 250 °C), iron oxy/hydroxides and kaolinites (dehydroxylation between 450 and 600 °C) using a Netzsch model STA409 PC (Karathanasis, 2008). Whole-rock major elements of seven laminar calcretes were determined at the SERNAGEOMIN (Chilean Geological Survey) laboratory by acid digestion/fusion using atomic absorption spectrophotometry and UV–visible spectrophotometry. Data were normalized to 100% on a loss on ignition (LOI) free basis. Soil development was evaluated in order to construct chronofunctions. Here we analyzed the redness index (RI) and structure index (SI) of Harden (1982) obtained from field data, and compared the clay content over time. obtained using a Rigaku model Ultima IV X/ray diffractometer with a Cu Kα1 target operating at 40 V and 40 mA. Subsequently, the KCl treated samples were heated for 2 h, first at 350 °C (350 treatment) and subsequently at 550 °C. The Mg saturated samples were then solvated with glycerol (glycerol treatment) in order to differentiate between vermiculite, chlorite and smectitic species (Whittig and Allardice, 1986). A semi-quantitative comparison of diffraction maxima at 1.42 nm (d-spacing) after different treatments was used to discriminate between vermiculite, chlorite and poorly crystalline smectites. Diffraction maxima at 0.720 nm and 0.445 nm after KCl treatment and disappearance after heating were used to determine the presence of kaolinite. The presence of micas was determined using diffraction maxima at 1.01–0.99 nm and 0.33. In order to differentiate between trioctahedral and dioctahedral micas we performed low speed powder diffraction XRD analysis of selected samples withangles between 59.0 and 62.02. We used a low intensity peak at0.150 nm to determine the presence of muscovite (Fanning et al.,1989). Additionally, selected representative samples were subjected to differential scanning calorimetry (DSC) to detect the presence of smectites (dehydration between 25 and 250 °C), iron oxy/hydroxides and kaolinites (dehydroxylation between 450 and 600 °C) using a Netzsch model STA409 PC (Karathanasis, 2008). Whole-rock major elements of seven laminar calcretes were determined at the SERNAGEOMIN (Chilean Geological Survey) laboratory by acid digestion/fusion using atomic absorption spectrophotometry and UV–visible spectrophotometry. Data were normalized to 100% on a loss on ignition (LOI) free basis. Soil development was evaluated in order to construct chronofunctions. Here we analyzed the redness index (RI) and structure index (SI) of Harden (1982) obtained from field data, and compared the clay content over time.

4. Results

4.1. Soil-terrace relationships

Calcrete is present in five of the seven studied profiles in all terraces except the youngest soil, which is located in the Holocene terrace. The three soil profiles described on the TII terrace reached stage VI of Machette's (1985) sequence of calcrete development, which corresponds to the most advanced calcrete development stage. The Almendros and El Rincon profiles, located on the TIII and TIV terraces, respectively, reached stage V of calcrete development.
All the profiles showing an advanced stage of calcrete development are located on carbonate substrates, which are marine transgression deposits (Maitencillo, La Montosa, Alamito, and El Rincón profiles) or belong to the Coquimbo Formation (Almendros profile). The Las Lomas profile shows carbonate mottles assigning it to stage I according to Machette (1985).

However, this profile is located on a clayey unit of the Coquimbo Formation, so that it cannot be used for a direct comparison between the soil profiles. The Holocene beach profile shows weak soil development with no pedogenic carbonate in the matrix. All profiles have an upper layer of eolian origin (hereafter referred to as topsoil) tentatively identified as such by Herm (1969) and subsequently confirmed by Pfeiffer et al. (2011), based on quartz grain surface texture analysis as observed under a scanning electron microscope (SEM). The older Maitencillo profile, located near the inland border of the TII terrace, shows a Natric horizon with a high sodium exchange percentage and columnar structure (Table 2), and is therefore the only profile with calcrete that is classified as "Petrocalcid Solonetz" according to WRB (IUSS Working Group WRB, 2006) and as "Natric Petrocalcid" according to Soil Taxonomy (Soil Survey Staff, 2010). This profile is the only one containing calcrete that classifies differently from the other profiles in both classification systems used here (Fig. 2). The soils are Aridisols according to Soil Taxonomy, with the exception of the Holocene soil which is an Entisol due to its weak pedogenic development. According to the WRB, the soils are classified as Arenosol, Solonetz and Calcisol (Fig. 2).

4.2. Topsoil

All soils have an upper, unconformable layer, referred to here as topsoil. Four profiles were selected for quartz grain surface texture analysis by SEM, as described by Pfeiffer et al. (2011). These authors proposed an eolian origin for this topsoil and recognized different earlier transport processes as indicated by microfeature groups that reflect a similar type of motion in a specific transport medium (Bull, 1981; Higgs, 1979; Krinsley and Donahue, 1968; Mahaney, 2002). In all samples, up to three successive microfeature groups were distinguished in this way. The same analysis was used for the topsoil of the Las Lomas profile, which gave comparable results. All samples underwent the same processes reflecting first a high energy coastal environment, followed by eolian transport, and eventually silica precipitation and solution. In all studied samples, the grains show more than 90% of coastal environment features associated with periodic swash and backwash on a beach, although some grains show evidence of longer transport distances, perhaps during terrestrial runoff. All analyzed grains also show well-defined eolian transport and abrasion features, which increase with the soil age (Fig. 4a). The last process, represented by silica dissolution and precipitation, can be associated with pedogenic processes of weathering and clay illuviation.
Comparing some properties of the topsoil with the estimated profile age it is possible to obtain some functions indicating the soil evolution over time. There are many methods available to determine soil development, e.g. using field data to construct chronofunctions (Sauer, 2010). Here we analyzed the redness index (RI) and structure index (SI) of Harden (1982) obtained from field data, together with laboratory data such as the clay content. Soil color properties such as hue and chroma change during soil evolution, in a process known as rubification (Kubiena, 1970), which is associated with the synthesis of iron oxides (Schwertmann, 1993). The average RI (Harden, 1982) of the topsoil shows that rubification increases with age at Tongoy (Fig. 4b). This process is favored in a Mediterranean climate where humid winters induce chemical weathering and dry summers allow precipitation of iron oxides (Torrent et al., 1980). The structure index of Harden (1982) shows the structural evolution of the soils over time (Fig. 4c) and there is also an increase in the clay content with soil age (Fig. 4d). Micromorphological analysis of the topsoil shows different stages of mineral weathering and pedofeatures with increasing soil profile age. The youngest profile shows little sign of soil development with minor weathering of minerals and initial stages of clay formation, whereas the older soil profiles show an increase in clay coatings and iron nodules as well as weathering features of siliciclastic grains. Carbonate accumulation in the form of masses and fractions of laminar and massive calcrete within the topsoil are also present. In some profiles there are shell fragments at the soil surface and near burrows of the

rodent Spalacopus cyanus, which is widely distributed in the area and is known for its adaptation to hard soils (Bozinovic et al., 2005). Bioturbation of hard soils such as calcretes by burrowing rodents has been also reported in the United States (Brock and Buck, 2009; Hirmas and Allen, 2007; Johnson and Johnson, 2004).

The topsoil horizons' oriented clay XRD patterns of the studied profiles show a mixture of primary (i.e. quartz, muscovite, biotite) and secondary minerals (kaolinites, vermiculites, etc.). Figs. 5 and 6 show an XRD pattern comparison of surface and subsurface horizons of each terrace, respectively. The three soil profiles studied on the oldest terrace (Alamito, La Montosa and Maitencillo) present a clay mineralogy dominated by muscovite and kaolinite. According to our DSC analysis the Bw horizon of La Montosa exhibits significantly higher contents of Fe oxides/hydroxides (probably goethite with an endothermic area between 300 and 400 °C) and kaolinites (500–600 °C), than any other of the analyzed soil horizons. The Bw/Bkm horizon of La Montosa is the only soil of this age that presents a peak for vermiculites. On the other hand, the Los Almendros soil (TIII) presents a mineralogy dominated by poorly crystalline smectites as well as vermiculites, chlorites and kaolinite. The mineralogy of the Las Lomas profile, which represents an intermediate state of development, is dominated mainly by poorly crystalline smectites, vermiculite, muscovite and kaolinites. This profile presents a significant increase in peak intensity for vermiculite and poorly crystalline smectites in the two deepest horizons (2Bt3 and 3C). Similarly, kaolinite shows a relatively higher peak intensity in these two horizons. This relative content increase was also corroborated by means of DSC analysis, which shows a clear endothermic area in the 450–600 °C range. The topsoil of the youngest terrace (TV) shows an XRD pattern similar to that of the Las Lomas soil, but with significantly higher intensities for vermiculite and kaolinites in the surface horizons (A and BC1) (Fig. 5). However, based on the DSC analysis the relative amounts of kaolinite in the youngest soil are significantly lower than that found on the Las Lomas Bw horizon.

4.3. Calcrete

Soil profiles with calcrete were observed at Tongoy only in areas with biogenic carbonate deposits. These calcretes comprise highly indurated calcium carbonate horizons and correspond to petrocalcic horizons (Soil Survey Staff, 2010). Calcrete is locally known as “losa” (Paskoff, 1970). The sediments of these soil profiles are associated with seaward-prograding beach ridges that developed after the marine transgressions abraded the terraces (Fig. 7). The only profile showing a calcrete developing directly from deposits of the Coquimbo Formation is at the top of a stratigraphic sequence at Almendros, described by Olivares (2004), which was Sr-dated at 1.4±0.5 Ma. However, the terrace level of the Almendros profile is associated with MIS 7e (about 225 ka BP) when the terrace was formed by abrasion. Calcrete profiles of the oldest level (TII terrace), show a sequence of an eolian topsoil underlain by brecciated calcrete, which overlies a laminar calcrete capping a massive calcrete.

Laminar calcrete shows tepee structures and pisolithic layers, which correspond to the most advanced stage of calcrete development according to Machette (1985). There are no considerable differences between the calcretes of the three profiles studied in the older TII terrace. Pfeiffer et al. (2011), showed that at first a massive calcrete developed in which many biogenic microfabric features were present (beta type), subsequently a laminar calcrete developed in which precipitation was mainly related to physiochemical processes (alpha type). The presence of gypsum and halite in the lower parts of the massive calcrete was interpreted as reflecting periods of high evaporation rates (Pfeiffer et al., 2011) (Fig. 8a). Clay coatings in the lower parts of the laminar calcrete along the contact with massive calcrete

reflect clay translocation before the formation of the laminar calcrete (Pfeiffer et al., 2011). Clay coatings and carbonate hypo-coatings are also present in the Las Lomas profile (Fig. 8b, c, respectively), where they are associated with high ESP (exchangeable sodium percentage) levels. Calcretes of profiles Almendros (TIII — 225 ka) and El Rincón (TIV — 123 ka) show a sequence of eolian topsoil, underlain by a laminar calcrete and massive calcrete, both profiles corresponding to stage V of calcrete development according to Machette (1985). The laminar calcretes are separated by thin pisolithic horizons (Fig. 8d). No clear differences in the stage of calcrete development are observed between profiles of the TIII and TIV terraces, despite the age differences between them. The microfabric of massive calcrete in both profiles shows an alveolar septal structure (Fig. 8e), which is related to fungal septa (Goldstein, 1988; Wright, 1986; Wright and Tucker, 1991). However, the presence of equant cement at Almendros suggests that diagenetic processes could have cemented the massive calcrete during its initial stages of development, which was subsequently eroded and exposed to pedogenic processes with biological activity so that laminar calcrete developed. At the El Rincón profile, ooliths and peloids are abundant in some layers of massive calcrete, which could be the result of calcification of fecal pellets in a carbonate substrate (Fig. 8f; Braithwaite, 1983; Calvet and Julia, 1983; Klappa, 1978).

The laminar calcrete shows similar macrostructures and microfabric patterns in the five calcrete profiles analyzed. It overlies the massive calcrete as a continuous layer composed of a series of microlaminations with variable Munsell colors. It lies between 33 and 70 cm depth. Locally, where the substrate is richer in siliciclastic deposits, carbonate precipitated as interlacing laminations or honeycomb calcrete and macroscopic rhizoliths are locally present (Fig. 9; Wright and Tucker, 1991). The upper part of the laminar calcrete is composed of four to five microlaminae with different microstructures between them. Normally the upper microlaminae present an undulating pattern, but they may also show microfractures with microsparite cement (Fig. 10a). The microlaminae are composed of pure secondary carbonates of micrite and microsparite, locally containing siliciclastic or bioclastic grains (Fig. 10b). Pisoids and ooliths were also observed (Fig. 10c). At some profiles on terraces TII and TIV, paleochannels cutting into calcrete are present, for example at terrace TIV where they eroded the first sequence of laminar and massive calcrete, leaving the underlying calcretes intact (Fig. 11). These profiles do not show calcrete development along the former channel surface. The whole-rock chemical composition of the upper microlaminae in the laminar calcretes at El Rincón (123 ka), Almendros (225 ka) and La Montosa (370 ka) shows an increase in the Si content, as well as a relative increase in Fe content of the oldest profiles (Table 3).

5. Discussion

The studied soil chronosequence indicates different stages of soil development on the different terraces and also between the soils of the large TII terrace. Depending on the stage of soil formation, the eolian cover of the Tongoy soils, also shows differences in its structure, redness index (Harden, 1982), and clay content. Moreover, calcretes of older terrace TII profiles demonstrate a more advanced formation stage in comparison with the TIII and TIV profile, as shown in Fig. 12. After the marine regression of MIS 11, gypsum and halite precipitation may have occurred as a consequence of high evaporation rates, which could be preserved in the lower parts of the deposit due to subsequent cementation forming the massive calcrete (Fig. 12). This process occurred in the three soil profiles of terrace TII, but no evidence thereof is found in younger profiles on this terrace studied by Vera (1985) and Aburto et al. (2008). This suggests that such arid conditions occurred shortly after the onset of the marine regression, related to a vadose zone with brackish water, as suggested by the presence of calcite columnar cement microfeatures (Adams et al., 1984). The presence of brackish waters in coastal areas is commonly related to deficient freshwater recharge

(Kocurek, 1996). The formation of the massive calcrete on the oldest terrace was driven by inorganic and biogenic processes, the latter being manifested as rhizoliths, peloids, alveolar septal structures, and some structures similar to fungal conidia. This implies that a vegetation cover existed at that time, which allowed the formation of these microstructures in the calcrete; biomass was probably composed mainly of grasses as suggested by the near absence of larger rhizoliths and the presence of gypsum and halite indicating scarce rainfall. The distribution of kaolinite does not show a clear pedogenic threshold. Since kaolinite is expected after intensive weathering processes (Murray and Keller, 1993) we may expect an increase with increasing soil development. This apparent incongruence may indicate kaolinitic parent materials or continuous additions of kaolinite-rich eolian sediments. The latter possibility is supported by relatively higher amounts of kaolinite in the surface horizon (Fig. 5) relative to the deeper horizons in all studied soils (Fig. 6). It is important to note that the greatest absolute amounts of kaolinite in the clay fractions were found in the Los Almendros Bw1 horizon (TIII). This may suggest that added neosynthesized kaolinites have been preserved in this system. The Los Almendros profile (TIII) also presents the highest intensity for vermiculite. This mineral is also abundant in the youngest profile, while it is practically absent from other, older profiles (Alamito and La Montosa). The presence of vermiculite in the youngest profile (TV) could be the result of parent material inheritance, since it is a mineral that is formed from the action of supergene solutions on biotite (De La Calle and Suquet, 1988), a mineral common in the rocks of the area (Emparan and Pineda, 2006). However, it is also possible that vermiculites were formed in situ as a result of pedogenic biotite alteration. The analysis of powder nonoriented samples shows that both biotite and muscovite are present in the youngest soil (TV), while only muscovite is present in the three older soils (TII). The reduction in muscovite peak intensity in Los Almendros (TIII) along with an increase in vermiculite peak intensity may indicate enhanced alteration of muscovite to dioctahedral vermiculite in this soil. The relatively faster alteration of biotite to trioctahedral vermiculites may explain the presence of the latter in the youngest soil (TV) and the absence of the former in the more developed topsoils (TII). On the other hand, the preservation of muscovite in the more developed topsoils could also be a consequence of a relatively higher stability of muscovite with respect to biotite (Malström and Banwart, 1997). According to Fanning and Keramidas (1982) muscovite is generally found in association with kaolinite when the soil solution is supersaturated with Ca and Si under a high pH. Our chemical analyses suggest that these conditions may be present in the studied soils, supporting the preservation of muscovite in older profiles. The highest relative amounts of chlorite are present in the youngest soil, whereas there is no chlorite in the clay fraction at Alamito and La Montosa, suggesting that chlorite may have been altered to vermiculite. In summary, as the topsoil developed, biotite along with other 2:1 and 2:1:1 clay mineral components tended to disappear, whereas muscovite and kaolinite tended to be preserved within this sequence. Clay films in the upper part of massive calcrete on the TII terrace suggest weathering and clay formation in the sandy upper eolian layer, and that the rainfall increased to a level sufficient for clay illuviation as shown by micromorphological features in the Alamito and La Montosa profiles. The presence of impure clay pedofeatures has been explained to result from the impairment of the parallel orientation of clay platelets induced by the disruption of both clay and silt-size layer silicates in a Na-rich environment (Pal et al., 1994).

Clay pedofeatures alternating with $CaCO_3$ coatings have also been understood to result from climate change (Gile et al., 1966; Reheis, 1987; Reynders, 1972; Yarilova, 1964). Pal et al. 2003) reported that clay illuviation and the formation of $CaCO_3$ in highly Na-rich soils from India occur simultaneously in a moist, ustic soil regime. According to these authors, this can occur when a high amount of sodium causes precipitation of soluble Ca^{2+} ions as calcium carbonate ($CaCO_3$), preventing the flocculation of clay by Ca^{2+}. The impure clay pedofeatures, high amounts of Na, and a low Ca/Na ratio match our results for the Maitencillo

profile (Table 2). The other two profiles of TII show different clay illuviation features and ESP (Exchange Sodium Percentage); although due to the high mobility of cations in the soil, these values should be interpreted with caution. In these profiles, clay coatings below the laminar calcrete are well oriented and have a high birefringence. In addition to this, the Ca/Na ratios are higher than 1, while in the Maitencillo profile the highest value is 0.07. These differences in the Ca/Na ratio may explain the different precipitation of clay coatings in these profiles. In the Alamito and Montosa profiles, thin coatings along the rims of grains were emplaced before carbonate precipitated in the pore spaces between the grains. Clay coatings engulfed by carbonates are interpreted as reflecting a climate change from wet to dry (El-Tezhani et al., 1984; Reheis, 1987). However, Bronger and Sedov (1997) and Cabadas et al. (2010) proposed an alternative model for clay coating formation in soils of semi-humid tropical or Mediterranean climates, which does not require climate change or the presence of exchangeable Na. When a leached Bt or Bw horizon is present overlying a petrocalcic horizon or calcareous bedrock, suspended clay mobilized in the leached upper horizons can be translocated downward and precipitated along carbonate contacts at the leaching front. However, the fact that these illuvial pedofeatures are separated from the present Bw horizon by continuous laminar crusts, excludes their recent origin. It is also important to note that the presence of brecciated calcretes implies the prior formation of a laminar calcrete, so that the time span between the formation of massive calcrete and clay illuviation could be significant.
Despite the lack of age control of the soil components, it is clear that the eolian layer was deposited previous to the formation of the laminar calcrete, as indicated by the presence of clay films along the contacts between laminar and massive calcrete. The different stage of soil development in this layer shows that it was also deposited after surface exposure subsequent to the marine regression. The quartz grain surface textures indicating a coastal environment confirm the coastal source of the sand, which was derived from sources feeding the five valleys debouching into the Bay of Tongoy. The increase in the proportion of well-abraded grains transported by wind with profile age indicates continuous reworking of sand until it was stabilized and started forming soil. The characteristics of the sand cover at Tongoy meet those of sand sheets, where dunes with slipfaces are generally absent (Kocurek, 1996).
Calcretes of the Almendros (TIII — 225 ka) and El Rincón (TIV — 123 ka) profiles show a sequence of topsoil overlying a laminar calcrete above a massive calcrete (brecciated calcrete is absent). Laminar calcretes are composed of multiple laminae, separated by thin pisolithic horizons. These are associated with mature calcrete profiles that become indurated and suffer cracks where the grains are free to move and nucleate around host objects, preferentially roots (Wright, 1994). On the TIV terrace in a road-cut profile near the Tongoy River, a series of erosion and calcrete reprecipitation processes can be observed in two well-defined laminar and massive calcretes (Fig. 11). Radtke (1989) dated the laminar and massive calcretes of this profile, but the age ranges are too wide to be used with confidence. The importance of this profile is that in the time span between MIS 5e (123 ka) and the present, a massive plus a laminar calcrete reaching at least stage V (Machette, 1985) developed twice. These calcretes were also eroded by channels in which no new calcrete developed. This implies that calcrete development rates in the study area did not need the full time span required to reach stage V as reported from other areas under semi-arid climates such as southeast Spain (Mediterranean), where the mature stage required a time-span between 69 ka to 121 ka (Candy et al., 2004). At Tongoy, the controlling factors for calcrete formation existed for a significant period after MIS 5e, but apparently ended around the first occurrences of debris flow.

Analysis of the chemical composition of the upper microlaminae from the laminar calcretes of the El Rincón (123 ka), Almendros (225 ka) and La Montosa (370 ka) profiles shows a higher Si content in the oldest profiles (Table 3), as can be expected for mature calcretes where silica saturation should be higher than in younger calcretes (Milnes and Hutton, 1983; Nash and

Shaw, 1998). The association of calcrete and silcrete occurs in continental basins with arid and semi-arid climates (Arakel et al., 1989; Nash and Shaw, 1998; Summerfield, 1982; Watts, 1980). At Tongoy, the semi-arid Mediterranean climate could have induced the production of CO2 during the wet season by the breakdown of organic matter and root respiration. The introduction of CO2 to the soil solution would have resulted in a local reduction in soil pH that affected calcite solubility and induced silica precipitation (Knoll, 1985; Siever, 1962). Furthermore, an inverse solubility exists between calcite and silica at high pH levels, when calcite precipitates simultaneously with silica dissolution, in turn increasing the silica saturation in the soils (Goudie, 1983; Siever, 1962). The process of calcrete silification is considered to be an integral part of their formation when silica is released during the replacement of silicate minerals (Walker, 1960; Watts, 1980).

6. Correlation with paleoclimate data

Calcretes are known to develop under arid, semi-arid and Mediterranean climates with a prolonged dry season (Alonso-Zarza and Wright, 2010, and references therein). The more advanced calcrete development (stage VI) on the TII terrace in comparison to profiles on terraces TIII and TIV (stage V) indicates that calcrete development did not begin everywhere at the same time. Furthermore, early cementation of the carbonate profile in terrace II after the MIS 11 highstand is supported by: the preservation of microrelief (Pfeiffer et al., 2011), and of highly soluble mineral preservation (gypsum and halite), and the scarcity of rhizoliths. It is also highly possible that the existence of a hyper-arid climate after MIS 11 and the presence of a brackish vadose zone were followed by an arid or semiarid climate that led to the development of a stage V calcrete with a laminar horizon. Subsequently, brecciation of the laminar calcrete occurred and a more humid period commenced that allowed for weathering of the sand cover and clay illuviation. Finally, a new laminar calcrete horizon developed.

Similar conditions of aridity were also maintained after MIS 5e, where a stage V calcrete developed with similar characteristics of beta and alpha morphology for massive and laminar calcrete, respectively. Without absolute dating of the soil components it is unclear if the calcrete on the TIII terrace developed earlier than the TIV terrace calcrete, but the presence of superimposed massive and laminar calcrete on the latter terrace indicates the prevalence of arid climatic conditions for a long time after MIS 5e.

Paleochannels observed in the TII and TIV terraces could be related to occasional intense rainfall or debris flows such as recorded by Vargas et al. (2006) in the Atacama Desert for El Niño/Southern Oscillation events (ENSO). The absence of newly formed calcrete after the channel incision into the older calcrete on the TII and TIV terraces suggests either a change in climatic conditions that did not allow calcrete development or that the channel erosion was a more recent event that did not allow sufficient time for calcrete formation.

The clay mineralogy of the selected topsoil layers shows a clear tendency in the disappearance of vermiculite, chlorite and smectites with increasing relative age of soil profiles (Figs. 5 and 6). Surface horizons in the older profiles (TII) only show peaks for kaolinite, muscovite and quartz, indicating complete alteration of more weathering-prone minerals (i.e. biotite, chlorites, etc.). Interestingly, the subsurface Bw horizon in the La Montosa profile presents small peaks for dioctahedral vermiculite and a reduction in the peak intensity of muscovite. The highest peak intensities for vermiculite, smectite and chlorite were found in the subsurface horizons of Los Almendros (TIII). Since its deposition, this soil may have experienced conditions that initially favored alteration of biotite and a subsequent

condition that allowed its preservation. Some conditions that allow the preservation of these minerals are reduced drainage or a silica-enriched environment (Allen and Hajek, 1989).

The sandy layer that covers the terraces shows high energy processes associated with swashing on a beach, followed by eolian transport. Since the quartz grain surfaces show signs of beach processes, it is likely that the Tongoy beach was the source area. The clay content, rubification and structure of the sandy layer show a sequence of pedogenic development in the soils, suggesting that deposition could have occurred at different times in response to pulses of climatic conditions suitable for eolian transport.

Previous paleoclimatic studies of the Norte Chico proposed an alternation between arid and relatively humid phases occurring at least over the last 120 ka, which is related to the latitudinal displacement of the Southern Westerlies (Grosjean et al., 1997, 1998; Lamy et al., 1998, 2000; Maldonado and Villagrán, 2002, 2006; Veit, 1996; Villagrán and Varela, 1990). Up to now, no paleoclimatic records have been available for the Norte Chico region for periods preceding MIS 5e, but our results indicate that these alternating climate cycles go back to at least MIS 11.

Fig. 12 summarizes the main sedimentological and pedological processes that occurred in the Tongoy soil profiles of the TII and TIV terraces. The TIII terrace is not shown as this soil reached a similar stage to IV for the TII profiles. In the future these stages and their correlation with past climatic events can be studied using isotope and dating techniques.
Beach ridge deposits associated with marine regression can be dated using U series, ESR and U–Th disequilibria techniques on marine shells (McLaren and Rowe, 1996; Muhs et al., 1989). These methods can also be used to date specific features of massive and laminar calcrete, such as rhizoliths, pisoliths and laminae (Candy and Black, 2009; Candy et al., 2004; Küçükuysal et al., 2011; Ludwig and Paces, 2002). Gypsum and halite minerals can be dated by using U–Th series up to a maximum of 350 ka (Ku et al., 1998).

Isotopic methods pertaining to carbonate can also be applied in combination with absolute dating methods to determine the vegetation in the area at the time of calcrete development. δ13C records of pedogenic carbonates are powerful indicators of paleoecology, as the δ13C reflects the isotope composition of soil CO2, which is also representative of the vegetation present at the moment of carbonate precipitation (Amundson et al., 1994; Deocampo, 2010; Pustovoytov et al., 2007; Singhvi et al., 2010).

7. Conclusions

At Tongoy, located in the semi-arid region of Chile, four marine terraces (TII–TV) developed over marine sediments corresponding to the Coquimbo Formation were studied. These terraces correspond to wave-cut features that formed due to variations in the relative sea level associated with marine isotopic stages MIS 11 for TII, MIS 7e for TIII, MIS 5e for TIV, and MIS 1 for TV, according to previous studies.

Over the three older terraces (TII, TIII and TIV), a calcrete developed locally where the parent material was calcareous. Terrace TV does not show any calcrete development because of its young age.

According to Machete's (1985) stages of development, the Tongoy calcretes reached stage VI on terrace TII and stage V on terraces TIV and TIII.

In all the studied profiles where calcretes developed, massive calcrete is of the beta type, in which organisms played an important role in CaCO3 precipitation. In laminar calcrete of alpha origin, CaCO3 precipitated because of physiochemical processes.

The different stages of calcrete development on the respective terraces indicate that they developed during different periods, which implies that climatic conditions favored their development in the area from at least MIS 11 (412 ka) to MIS 5e (125 ka).

Soils in the Tongoy paleobay resulted from a series of sedimentological, geomorphological and pedogenic processes that responded to climatic cycles of arid and more humid periods. Previously, these climatic cycles have only been recorded in the area after MIS 5e. However, the presence of well-developed calcrete soil profiles shows a clear sequence of events that can be associated with arid and more humid periods in three marine terraces, the oldest of which reaches MIS 11, suggesting that climate cyclicity in this area is older than 100 ka.

These climatic cycles recorded in the Tongoy calcretes present an outstanding opportunity for future studies that could link datable pedological features with the pre-MIS 5e climate of the area, allowing a precise sequence of events to be established.

Acknowledgments

The first author is grateful to CONICYT and the Departamento de Postgrado y Postítulo of the Universidad de Chile, for a fellowship that supported this study. Jose Padarian is thanked for his valuable assistance during field work. We also thank Eligio Jiménez and Jaime Díaz for thin section preparation, Hugo Perez for physical soil analysis and Marysol Aravena for chemical soil analysis. Osvaldo Salazar is thanked for his comments on the manuscript. The original manuscript benefited greatly from the comments of two anonymous reviewers.

REFERENCES

Aburto, F., Hernández, C., Pfeiffer, M., Casanova, M., Luzio, W., 2008. Northern Field-Guide. The International Conference and Field Workshop on Soil Classification. Soil: A Work of Art of the Nature. Universidad de Chile, Santiago.

Adams, A.F., Mackenzie, W.S., Guilford, C., 1984. Atlas of Sedimentary Rocks under the Microscope. Longman, Wiley, New York-London.

Allen, B.L., Hajek, B.F., 1989. Mineral occurrence in soil environments, in: Dixon, J.B. and Weed, S.B. (Eds.), Minerals in Soil Environments. Second Edition, Soil Science Society of America Book Series, pp 199-278

Alonso-Zarza, A.M., Wright, V.P., 2010. Calcretes, in: Alonso-Zarza, A.M., Tanner, L.H. (Eds.), Carbonates in Continental Settings: Facies, Environments and Processes: Developments in Sedimentology, 61, Elsevier, Amsterdam, pp. 225-268.

Amundson, R., Wang, Y., Chadwick, O., Trumbore, S., McFadden, L., McDonald, E., Wells, S., DeNiro, M. 1994. Factors and processes governing the ^{14}C content of carbonate in desert soils. Earth and Planetary Science Letters 125, 385-405.

Anderson, R.S., Densmore, A.L., Ellis, M.A., 1999. The generation and degradation of marine terraces. Basin Research 11, 7-19.

Arakel, A.V., Jacobson, G., Salehi, M., Hill, C.M., 1989. Silicification of calcrete in palaeodrainage basins of the Australian arid zone. Australian Journal of Earth Sciences 36, 73-89.

Berger, I.A., Cooke, R.U. 1997. The origin and distribution of salts on alluvial fans in the Atacama Desert, northern Chile. Earth Surface Processes and Landforms 22, 581- 600.

Benado, D.E., 2000. Estructuras y Estratigrafía Básica de Terrazas Marinas en Sector Costero de Altos de Talinay y Bahía Tongoy: Implicancia Neotectónica. Memoria, Departamento de Geología, Universidad de Chile, Santiago de Chile.

Bouyoucos, G.J., 1936. Directions for making mechanical analyses of soils by the hydrometer method. Soil Science 42, 225-230.

Bozinovic, F., Carter, M.J., Ebensperger, L.A., 2005. A test of the thermal-stress and the cost-of-burrowing hypotheses among populations of the subterranean rodent *Spalacopus cyanus*. Comparative Biochemistry and Physiology A 140, 329-336.

Brock, A.L., Buck, B.J., 2009. Polygenetic development of the Mormon mesa, NV petrocalcic horizons; Geomorphic and palaeoenvironmental intepretations. Catena 77, 65-75.

Bronger, A., Sedov, S.N., 1997. Origin and redistribution of pedogenic clay in terrae rossae from Quaternary calcarenites in coastal Moroco, in: Shoba, S., Gerasimova, M., Miedema, R. (Eds.). Soil Micromorphology: Studies on Soil Diversity, Diagnosis, Dynamics. Moscow-Wageningen, pp. 59-66.

Braithwaite, C.J.R., 1983. Calcrete and other soils in Quaternary limestones: Structures, processes and applications. Journal of the Geological Society of London B273, 1 – 32.

Brüggen, J. 1950. Fundamentos de la Geología de Chile. Instituto Geográfico Militar, Santiago de Chile.

Bull, P.A., 1981. Environmental reconstruction by scanning electron microscopy. Progress in Physical Geography 5, 368-397.

Bullock, P., Fedoroff, N., Jongerius, A., Stoops, G., Tursina, T., Babel., U., 1985. Handbook for Soil Thin Section Description. Waine Research Publications. Wolverhampton, U.K.

Cabadas, H., Solleiro-Rebolledo, E., Sedov, S., Pi, T., Alcalá, J.R., 2010. The complex génesis of Red Soils in Peninsula Yucatan, Mexico: Mineralogical, micromorphological and geochemical proxies. Eurasian Soil Science 13, 1439-1457.

Calvet, F., Julia, R., 1983. Pisoids in the calcite profiles of Tarragona, north-east Spain, in: T.M. Peryt (Ed.), Coated Grains. Springer Verlag, Berlin, pp. 456-473.

Candy, I., Black, S., 2009. The timing of Quaternary calcrete develpment in semi-arid southeast Spain: Investigating the role of climate on calcrete génesis. Sedimentary Geology 218, 6-15.

Candy, I., Black, S., Sellwood, B.W., 2004. Quantifying time scales of pedogenic calcrete formation using U-series disequilibria. Sedimentary Geology 170, 177-187.

Casanova, M., Seguel, O., Luzio W., 2010. Suelos de la zona Árida y Semiárida (desde 29° S hasta 32° S). In: Luzio, W. (Ed.), Suelos de Chile. Universidad de Chile, pp. 81-123.

Chávez, C., 1967. Terrazas de abrasión. In: Thomas, H. (Ed.), Geología de la Hoja Ovalle, Provincia de Coquimbo. Instituto de Investigaciones Geológicas, Boletín 324, 137-140.

Cerling, T., Quade, J., 1993. Stable carbon and oxygen isotopes in soil carbonates. Climate change in continental isotopic records. Geophysical Monograph 78, 217-231.

CIREN, 1990. Atlas Agroclimático de Chile, Regiones IV a IX. Ministerio de Agricultura de Chile. Centro de Información sobre Recursos Naturales, Publicacion Nº 87, Santiago, Chile.

Cuevas, P., Vega, H., 2006. Análisis económico histórico y presente de la ganadería ovina en la Hacienda "El Tangue". Memoria, INACAP, La Serena, Chile.

Darwin, C., 1846. Geological Observations on South America. Smith, Elder and Co, London.

De La Calle, C.J., Suquet, D.H., 1988. Vermiculite, in: Nailey, S.W. (ed.). Hydrous phylosilicates (exclusive of mica). Reviews in Mineralogy 19. Mineralogical Society of America, Washington, DC, pp. 201-209.

Deocampo, D.M., 2010. The Geochemistry of Continental Carbonates. In: Alonso-Zarza, A.M., Tanner, L.H. (Eds.). Carbonates in Continental Settings: Geochemistry, Diagenesis and Applications. Developments in Sedimentology 62, Elsevier, Amsterdam, pp. 1-59.

Domeyko, I., 1848. Mémoire sur le terrain et les lignes d´ancien niveau de l´Océan du sud, aux environs de Coquimbo (Chili). Ann. Mines, 14, 153-162.

Durand, N., Monger, H.C., Canti, M.G., 2010. Calcium carbonate features. In: Stoops, G., Marcelino, V., Mees, F. (Eds.). Interpretation of Micromorphological Features of Soils and Regoliths. First Edition. Elsevier, Amsterdam.

El-Tezhani, M.S., Gradusov, B.P., Rubilinia, N., Ye., Chizikova, N.P., 1984. Chemical and mineral composition of the finely dispersed component and microstructure of some soils in Sudan. Soviet Soil Science 16, 75-81.

Emparan, C., Pineda, G., 2006. Geología del Área Andacollo-Puerto Aldea, Región de Coquimbo. Escala 1:100.000. Servicio Nacional de Geología y Minería, Serie Geología Básica 96, Santiago, Chile.

Fanning, D.S. and Keramidas, V.Z., 1982. Micas, in: Dixon and Weed (Eds.), Minerals in soil environments . Soil Science Society of America (SSSA). Madison, Wisconsin, USA.

Fanning, D.S., Keramidas, V.Z., El-Desoky, M.A., 1989. Micas, in: Dixon, J.B. and Weed, S.B. Minerals in soil environments. Second Edition. Soil Science Society of America Book Series, pp 551-634.

Franz, H., 1966. Qartäre Sedimente und Böden in Chile und Argentinien sowie ihre Bedeutung für die biogeographische Forschung. Revista Ecol. Biol. Sol. 3, 355-379.

Fuenzalida, H., 1951. Pedalfers en el Norte Chico y sus relaciones con relictos vegetacionales. Informaciones Geográficas 3-4, 62-64.

Gajardo, R., 1994. La Vegetación Natural de Chile. Clasificación y Distribución Geográfica. Editorial Universitaria, Santiago, Chile.

Gile, L.H., Petersen, F.F., Grossman, R.B. 1966. Morphological and genetic sequences of carbonate accumulation in desert soils. Soil Science 101, 347-360.

Gocke, M., Pustovoytov, K., Kühn, P., Wiesenberg, G., Löscher , M., Kuzyakov, Y. 2011. Carbonate rhizoliths in loess and their implications for paleoenvironmental reconstruction revealed by isotopic composition: $\delta^{13}C$, ^{14}C. Chemical Geology. 283 (3-4), 251-260.

Goldstein, R.H., 1988. Palaeosols of Late Pennsylvanian cyclic strata, New Mexico. Sedimentology 35, 777-804.

Goudie, A.S., 1983. Calcretes, in: Goudie, A.S., Pye, K. (Eds.), Chemical Sediments and Geomorphology. Academic Press, London, pp. 93-131.

Grosjean, M., Valero-Garcés, B.L., Geyh, M.A., Messerli, B., Schotterer, U., Schreier, H., Kelts, K., 1997. Mid- and late-Holocene limnology of Laguna del Negro Francisco, northern Chile, and its palaeoclimatic implications. The Holocene 7, 151-159.

Grosjean, M., Geyh, M.A., Messerli, B., Schreier, H., Veit, H., 1998. A late-Holocene (<2600 BP) glacial advance in the south-central Andes (29°S), northern Chile. The Holocene 8, 473-479.

Grossman, R.B, Reinchs, T.G., 2002. Bulk density and linear extensibility, in: Dane, J. H. and Topp, G. C. (Eds). Methods of Soil Analysis. Part 4: Physical Methods. SSSA Book Serie Nr 5. Madison, Wisconsin, USA., pp. 201-228.

Harden, J.W., 1982. A quantitative index of soil development from field descriptions: examples from a chronosequence in central California. Geoderma 28, 1-28.

Heinze, B., 2003. Active intraplate faulting in the forearc of north central Chile (30°S): Implications from neotectonic field studies, GPS data, and elastic dislocation modeling. Scientifical Technical Report, Geoforschungszentrum, Potsdam, Germany.

Herm, D., 1969. Marines Pliozän und Pleistozän in nord und mittel Chile unterbesonderer Berücksichtigung der Entwicklung der Mollusken Faunen. Zitteliana 2.

Higgs, R., 1979. Quartz surface features of Mesozoic-Cenozoic sands from Labrador and Western Greenland continental margins. Journal of Sedimentary Petrology 49, 599- 610.

Hirmas, D.R., Allen, B.L., 2007. Degradation of pedogenic calcretes in west Texas. Soil Science Society of America Journal 71, 1878-7888.

Hsu, J.T., Leonard, E.M., Wehmiller, J.F., 1989. Aminostratigraphy of Peruvian and Chilean Quaternary marine terraces. Quaternary Science Reviews 8, 255-262.

IUSS Working Group WRB. 2006. World Reference Base for Soil Resources 2006. World Soil Resources Report No. 103, FAO Rome.

Jackson, M.L. 1975. Soil Chemical Analysis – Advance Course. Second Edition. 10th printing. Published by the author, Madison, Wisconsin.

Johnson, D.L., Johnson, D.N., 2004. Bioturbation by badgers and rodents in producing polygenetic and polytemporal desert soil biomantles : soil formation, or soil evolution?. Geological Society of America Annual Meeting, Quaternary Geology. Abstracts Vol. 36, 97.

Karathanasis A.D. (2008). Thermal Analysis of Soil Minerals. In: Methods of Soil Analysis. Part % - Minerological Methods. UleryA.L. and Richard Dress, L. (Ed.) Soil Science Society of America. ISBN: 978-0-089118-846-9

Klappa, C.F., 1978. Morphology, Composition and Genesis of Quaternary Calcretes from the Western Mediterranean: A Petrographic Approach. PhD Thesis, Univ. Liverpool (Unpublished).

Knoll, A.H., 1985. Exceptional preservation of photosynthetic organisms in silicified carbonates and silicified peats. Philosophical Transactions of the Royal Society, London B311, 111-122.

Kocurek, G.A., 1996. Desert aeolian systems, in: Reading, H.G. (Ed.), Sedimentary Environments. Third Edition, Blackwell Science Ltd., Oxford, pp. 125-153.

Krinsley, D. H. and Donahue, J., 1968. Environmental interpretation of sand grain surface textures by electron microscopy. Geological Society of America Bulletin 79, 743-748.

Ku, T.L., Luo, S., Lowenstein, Li, J., Spencer, R.J., 1998. U-series chronology of lacustrine deposits in Death Valley, California. Quaternary Research 50, 561-275.

Kubiena, W.L., 1970. Micromorphological Features of Soil Geography. Rutgers University Press, New Brunswick.

Küçükuysal, C., Engin, B., Türkmenoğlu, A.G., Aydaş, C., 2011. ESR dating of caclrete nodules from Bala, Ankara (Turkey): Preliminary results. Applied Radiation Isotopes 69, 492-499.

Lamy, F., Hebbeln, D., Wefer, G., 1998. Late Quaternary cycles of terrigenous sediment input off the Norte Chico, Chile (27.5°S) and palaeoclimatoc implications. Palaeogeography Palaeoclimatology, Palaeoecology 141, 233-251.

Lamy, F., Klump, J., Hebbeln, D., Wefer, G., 2000. Late Quaternary rapid climate change in northern Chile. Terra Nova 12, 8-13.

Latorre, C., Quade, J., McIntosh, W.C., 1997. The expansión of C_4 grasses and global change in the late Miocene: Stable isotope evidence from the Americas. Earth and Planetary Science Letters 146, 83-96.

Latorre, C., Moreno, P.I., Vargas, G., Maldonado, A., Villa-Martínez, R., Armesto, J., Villagrán, C., Pino, M., Núñez, L., Grosjean, M., 2007. Late Quaternary environments and

palaeoclimate. In: Moreno T., Gibbons, W. (Ed.). The Geology of Chile. The Geological Society, London, U.K., pp. 309-328.

Le Roux, J.P., Olivares, D.M., Nielsen, S.N., Smith, N.D., Middleton, H., Fenner, J., Ishman, S.E., 2006. Bay sedimentation as controlled by regional crustal behaviour, local tectonics and eustatic sea level changes: Coquimbo Formation (Miocene-Pliocene), Bay of Tongoy, central Chile. Sedimentary Geology 184, 133-153.

Ludwig, K.R., Paces, J.B., 2002. Uranium-series dating of pedogenic silica and carbonate, Crater Flat, Nevada. Geochimica et Cosmochimica Acta 66, 487-506.

Machette, M.N. 1985. Calcic soils of the south western United States. Geol. Soc. Am. Special Paper 203, 1-21.

Mahaney, W.C., 2002. Atlas of Sand Grain Surface Textures and Applications. Oxford University Press, New York, 237 pp.

Maldonado, A., Villagrán, C., 2002. Palaeoenvironmental changes in the semiarid coast of Chile (~32°S) during the last 6200 cal years inferred from a swamp-forest pollen record. Quaternary Research 58, 130-138.

Maldonado, A., Villagrán, C., 2006. Climate variability over the last 9900 cal yr BP from a swamp forest pollen record along the semiarid coast of Chile. Quaternary Research 66, 246-258.

Malström, M. And Banwart, S. 1997. Biotite dissolution at 25C: The pH dependence of dissolution rate and stoichiometry. Geochemica and Cosmochimica Acta, Vol. 61, No.14, pp 2779-2799.

McLaren, S.J., Rowe, P.J., 1996. The reliability of uranium/series mollusk dates from the western Mediterranean Basin. Quaternary Science Reviews 15, 709-717.

Miller, A., 1976. The climate of Chile. In: Schwerdtferger, W. (Ed.), Climates of Central and South America.World Survey of Climatology, 12. Elsevier, Amsterdam, pp. 113-145.

Milnes, A.R., Hutton, J.T., 1983. Calcretes in Australia. In: Soils, an Australian Viewpoint. CSIRO/Academic Press, pp. 119-162.

Moraga, J., Olivares, J., 1993. Condiciones oceanográficas del área próxima a la costa frente a Coquimbo, Chile. Ocas. Facultad Ciencias del Mar. U.C. del Norte, Coquimbo, 2: 125-140.

Murray, H.H., Keller, W.D., 1993. Kaolins, kaolins and kaolins, in: Murray, H.H., Bundy, W.M., Harvey, C.C. (Eds.), Kaolin Genesis and Utilization. Special Publication 1. Clay Minerals Society, Boulder CO.

Muhs, D.R., Rosholt, J.N., Bush, C.A., 1989. The uranium trend dating method: principles and applications for southern California marine terrace deposits. Quaternary International 1, 19-34.

Nash, D.J., Shaw, P.A., 1998. Silica and carbonate relationships in silcrete-calcrete intergade duricrusts from the Kalahari of Botswana and Namibia. Journal of African Earth Sciences 27, 11-25.

Olivares, D.M., 2004. Evolución Miocena-Pleistocena de las sucesiones sedimentarias marinas de Bahía Tongoy, IV Región de Coquimbo. Memoria, Departamento de Geología, Universidad de Chile, Santiago de Chile.

Ota, Y., Paskoff, R., 1993. Holocene deposits on the coast of the north-central Chile: radiocarbon ages and implications for coastal changes. Revista Geológica de Chile 20, 25-32.

Ota, Y., Miyauchi, T., Paskoff, R., Koba, M., 1995. Plio-Quaternary terraces and their deformation along the Altos de Talinay, north central Chile. Revista Geológica de Chile 22, 89-102.

Pal, D.K., Kalbande, A.R., Deshpande, S.B., Sehgal, J.L., 1994. Evidence of clay illuviation on sodic soils of north western part of the Indo-Gangetic plains since the Holocene. Soil Science 158, 465-473.

Pal, D.K., Srivastava, P., Bhattacharyya, T. 2003. Clay illuviation in calcareous soils of the semiarid part of the Indo-Gangetic Plains, India. Geoderma 115, 177-192.

Paskoff, R. 1970. Recherches géomorphologiques dans le Chili semi'aride. Biscaye frères, Bordeaux. 420 pp.

Pfeiffer, M., 2011. Evolución y génesis de calcretas pedogénicas en la Paleobahía de Tongoy. Masters Thesis, Departamento de Geología, Universidad de Chile, Santiago de Chile.

Pfeiffer, M., Le Roux, J.P., Solleiro-Rebolledo, E., Kemnitz, H., Sedov, S., Seguel, O., 2011. Preservation of beach ridges due to pedogenic calcrete development in the Tongoy paleobay, Chile. Geomorphology 132, 234-248.

Pustovoytov, K., Schmidt, K., Parzinger, H. 2007. Radiocarbon dating of thin pedogenic carbonate laminae from Holocene archaeological sites. The Holocene. 17(6), 835-843.

Quade, J., Rech, J.A., Latorre, C., Betancourt, J., Gleeson, E., Kalin, M.T.K., 2007. Soils at the hyperarid margin: the isotopic composition of soil carbonate from the Atacama Desert, northern Chile. Geochimica et Cosmochimica Acta 71, 3772-3795.

Radtke, U., 1989. Marine Terrassen und Korallenriffe. Das Probleem der Qartären Meersiegelschankungen erlänter an Fallstudien aus Chile, Argentinien und Barbados. Düsseldorfer Geographische Schriften 27, Düsseldorf, Germany.

Regard, V., Saillard, M., Martinod, J., Audin, L., Carretier,S., Pedoja, K., Riquelme, R., Paredes, P., Hérail, G., 2010. Renewed uplift of the Central Andes Forearc revealed by coastal evolution during the Quaternary. Earth and Planetary Science Letters 297, 199-210.

Rech, J.A., Quade, J., Hart, W.S. 2003. Isotopic evidence for the source of Ca and S in soil gypsum, anhydrite and calcite in the Atacama Desert, Chile. Geochimica Et Cosmochimica Acta 67, 575-586.

Reheis, M., 1987. Climatic Implications of alternating clay and carbonate formation in semiarid soils of south-central Montana. Quaternary Research 27, 270-282.

Reynders, J.J. 1972. A study of argillic horizons in some soils of Morocco. Geoderma 8, 267-279.

Sadzawka A., Carrasco, M.A., Grez, R., Mora, M.L., 2004. Métodos de análisis recomendados para los suelos chilenos. Comisión de Normalización y Acreditación. Sociedad Chilena de la Ciencia del Suelo.

Saillard, M., 2008. Dynamique du soulèvement côtier des Andes centrales: Etude de l´évolution géomorphologique et datations (^{10}Be) de séquences de terrases marines (Sud Pérou-Nord Chili). Ph.D Thesis, Université de Toulusem Toulouse.

Saillard, M., Hall, S.R., Audin, L., farber, D.L., Hérail, G., Martinod, J., Regard, V., Finkel, R.C., Bondoux, F., 2009. Non-steady long-term uplift rates and Pleistocene marine terrace development along the Andean margin of Chile (31°S) inferred from ^{10}Be dating. Earth and Planetary Science Letters 277, 50-63.

Sauer, D., 2010. Approaches to quantify progressive soil development with time in Mediterranean climate - I. Use of field criteria. Journal of Plant Nutrition and Soil Science 173, 822-842.

Schoenberger, P.J., Wysocki, D.A., Benham, E.C., Broderson, W.D., 2002. Field Book for Describing and Sampling Soils, Version 2.0. Natural Resources Conservation Service, National Soil Survey Center, Lincoln, NE.

Schwertmann, U., 1993. Relations between iron oxides, soil color, and soil formation. In: Bigham, J.M. and Ciolkosz, E.J. (Eds.), Soil Color, Soil Science Society of America Special Publication No 31, Madison, WI, USA.

Sidall, M., Chapell, J., Potter, E.K., 2006. Eustatic sea-level during past interglacials. In: Sirocko, F., Litt, T., Claussen, M., Sanchez-Goni, N.F. (Eds.), The Climate of Past Interglacials. Elsevier, Amsterdam.

Siever, R., 1962. Silica solubility 0-200°C and the diagenesis of siliceous sediments. Journal of Geology 70, 127-150.

Singhvi, A., Williams, M., Rajaguru, S., Misra, V., Chawla, S., Stokes, S., Chauhan, N., Francis, T., Ganjoo, R., Humphreys, G. 2010. A 200 ka record of climatic change and dune activity in the Thar Desert, India. Quaternary Science Reviews. 29 (23-24), 3095-3105.

Soil Survey Staff, 2010. Keys to Soil Taxonomy. 11th Edition. Washington, DC, Natural Resources Conservation Service, United States Department of Agriculture.

Stoops, G., 2003. Guidelines for Analysis and Description of Soil and Regolith Thin Sections, Soil Science Society of America, Madison.

Summerfield, M.A., 1982. Distribution, nature and probable genesis of silcrete in arid and semi-arid Southern Africa, in: Yaalon, H.D. (Ed.), Aridic Soils and Geomorphic Processes. Catena Supplement 1, Braunschweig, pp. 37-65.

Tanner, L.H., 2010. Continental carbonates as indicators of paleoclimate, in: Alonso- Zarza, A.M., Tanner, L.H. (Eds.), Carbonates in Continental Settings: Facies, Environments and Processes: Developments in Sedimentology, 61, Elsevier, Amsterdam, pp. 179-214.

Torrent, J., Scwertmann, U., Schulze, D.G., 1980. Iron oxide mineralogy of some soils of two river terrace sequences in Spain. Geoderma 23, 191-208.

Vargas, G., Rutlant, J., Ortlieb, L., 2006. ENSO tropical-extratropical climate teleconnections and mechanisms for Holocene debris flows along the hyperarid coast of western South America (17°-24°S). Earth and Planetary Science Letters 249, 467-483.

Veit, H., 1996. Southern Westerlies during the Holocene deduced from geomorphological studies in the Norte Chico, northern Chile (27-33°S). Palaeoecology, Palaeoclimatology, Palaeoecology 123, 107-119.

Vera, W., 1985. Mineralogy and Micromorphology of Calcium Carbonate-rich Soils from Chile. M.Sc. Thesis. State University of Ghent, Belgium.

Villagrán, C., 2007. Dinámica costera en el sistema de bahías comprendidas entre Ensenada Los Choros y Bahía Tongoy. Memoria para optar al título de geógrafo. Universidad de Chile.

Villagrán, C., Varela, J., 1990. Palynological evidence for increased aridity on the central Chilean coast during the Holocene. Quaternary Research 34, 198-207.

Villagrán, C., Armesto, J., Hinojosa, L.F., Cuvertino, J., Pérez, C., Medina, C., 2004. El enigmático origen del bosque relicto de Fray Jorge. In: Squeo, F.A., Gutiérrez, J.R., Hernández, I.R. (Eds.). Historia Natural del Parque Nacional Bosque Fray Jorge. Ediciones Universidad de La Serena, La Serena, Chile, pp. 3-43

Walker, T.R., 1960. Carbonate replacement of detrital crystalline silicate minerals as a source of authigenic minerals in sedimentary rocks. Bulletin of the Geological Society of America 71, 145-452.

Watts, N.L., 1980. Quaternary pedogenic calcretas from the Kalahari (Southern Africa): mineralogy, genesis and diagenesis. Sedimentology 27, 661-686.

Whittig, L.D., Allardice, W.R. 1986. X-ray diffraction techniques. p. 331–362 In A. Klute (Ed.) Methods of soil analysis. Part 1. 2nd ed. Agron. Monogr. 9. ASA and SSSA, Madison, WI.

Wright, C.S., Espinoza, J., 1962. Environment and soil-process in the Chilean sector of the west coast of South America. Transactions of the International Soil Conference, New Zealand, Comm.. IV y V, pp. 2-12.

Wright, V.P., 1986. The role of fungal biomineralisation in the formation of early Carboniferous soil fabrics. Sedimentology 33, 831-149.

Wright, V.P., 1994. Paleosols in shallow marine carbonate sequences. Earth-Science Reviews 35, 367-395.

Wright, V.P., Tucker, M.E., 1991. Calcrete: and introduction. International Association of Sedimentologists, Reprint Series 2, 1-22.

Yaalon, D.H., 1997. Soils in the Mediterranean region: what makes them different? Catena 28, 157-169.

Yarilova, E.A. 1964. Comparative micromorphological characteristics of some Solonetz soils of the Steppe semi-desets zones. In: Jongerius, A. (Ed.), Soil Micromorphology. Elsevier, New York, pp. 313-323.

FIGURE CAPTIONS

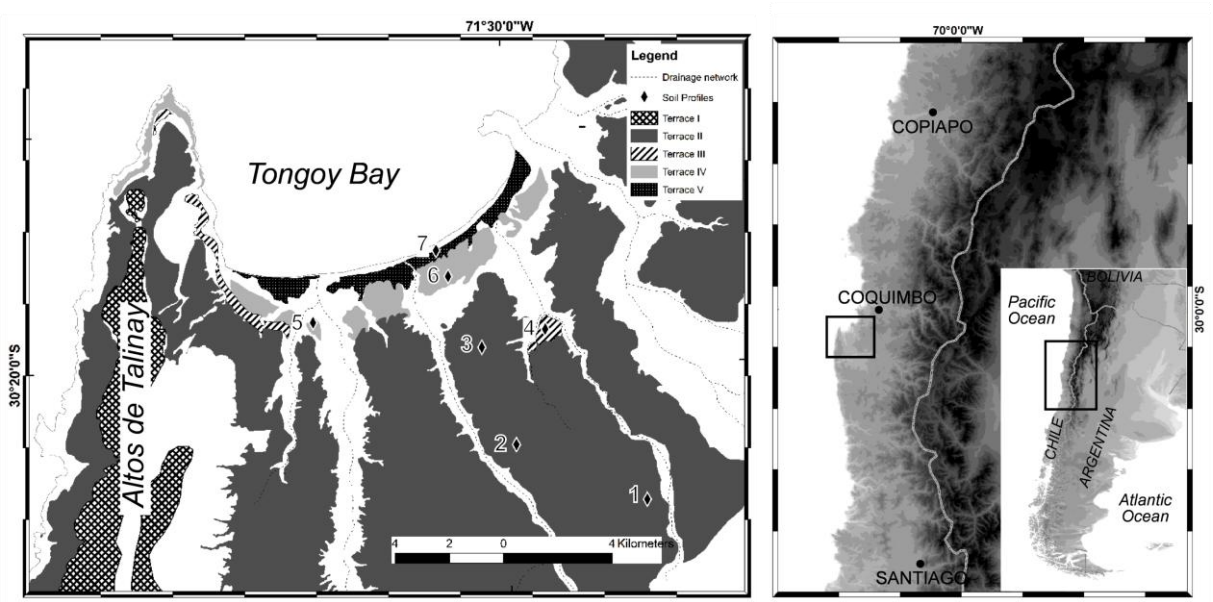

Figure 1. Location of the study area and distribution of soil profiles over marine abrasion terraces at Tongoy. Numbers represent soil profiles: 1, Maitencillo; 2, La Montosa; 3, Alamito; 4, Almendros; 5, El Rincón; 6, Las Lomas; 7, Beach.

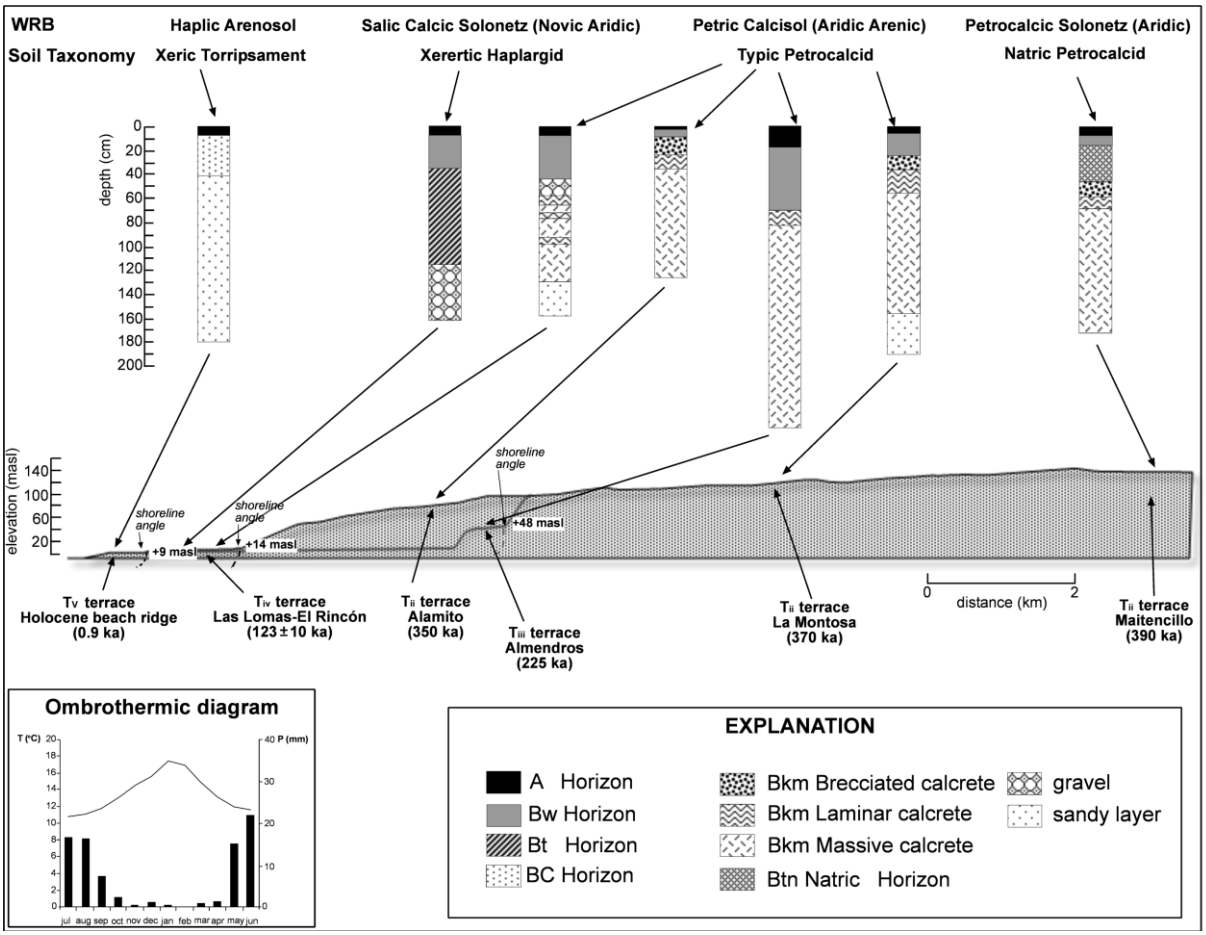

Figure 2. Soil profiles showing general stratigraphy, classification and relative topographic and geomorphological distributions. Ombrothermic diagram at left bottom.

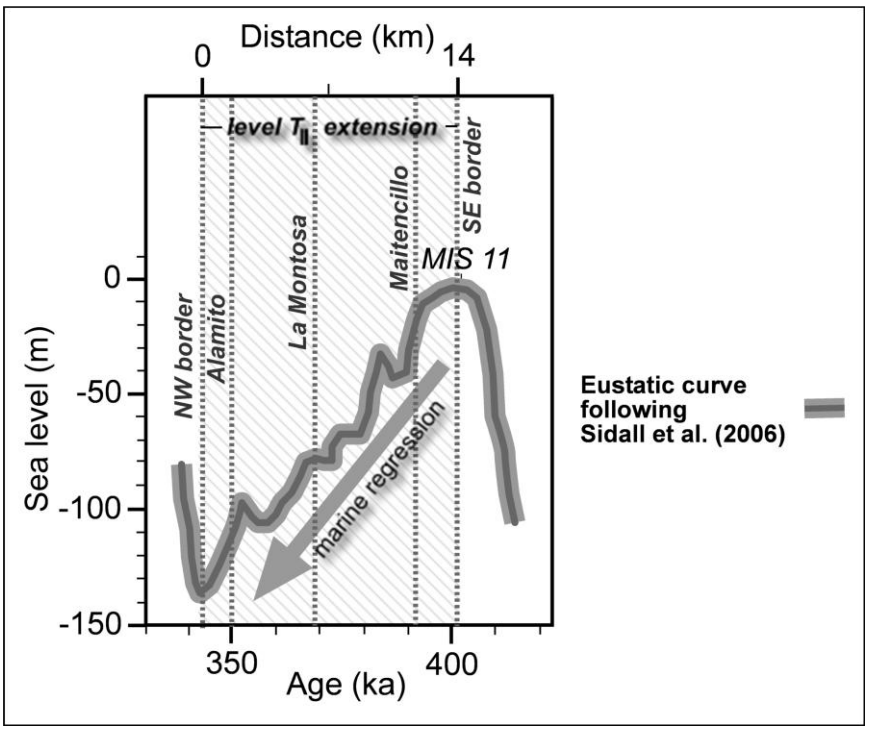

Figure 3. Sea level curve around the MIS 11 and relative soil profile ages according to their positions on terrace TII. The SE border should coincide with the MIS 11 highstand, whereas the NW border should coincide with the following sea level lowstand.

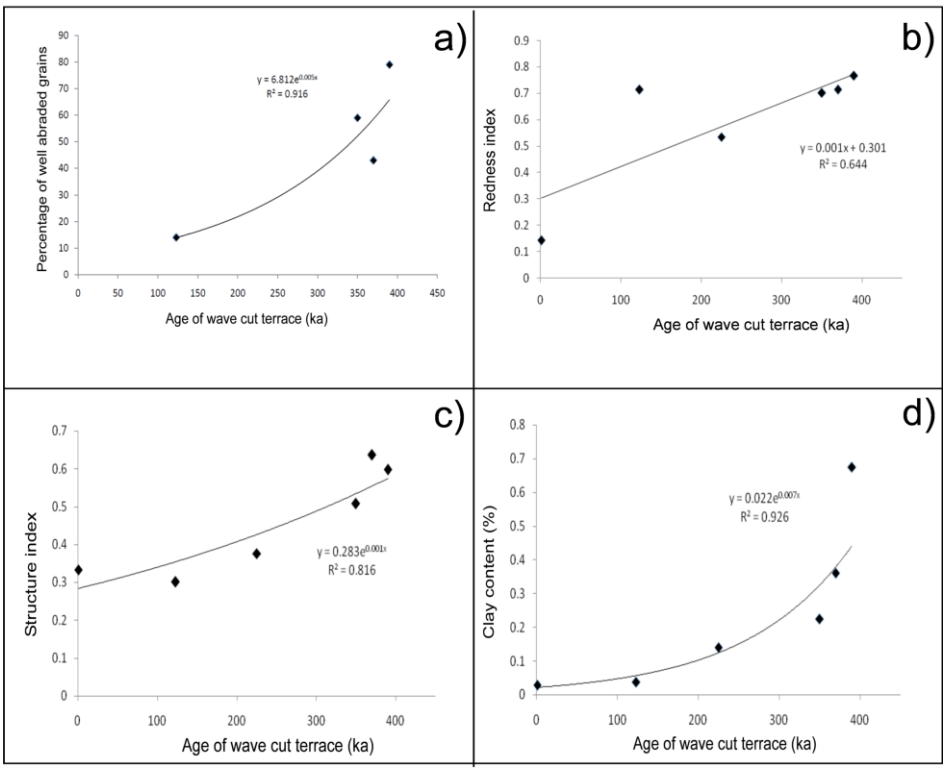

Figure 4. Soil properties of the upper eolian cap according to the surface age. a) Soil age v/s the percentage of well-abraded quartz sand grains; b) Redness index chronosequence; c) Structure index chronosequence; d) Topsoil clay content chronosequence.

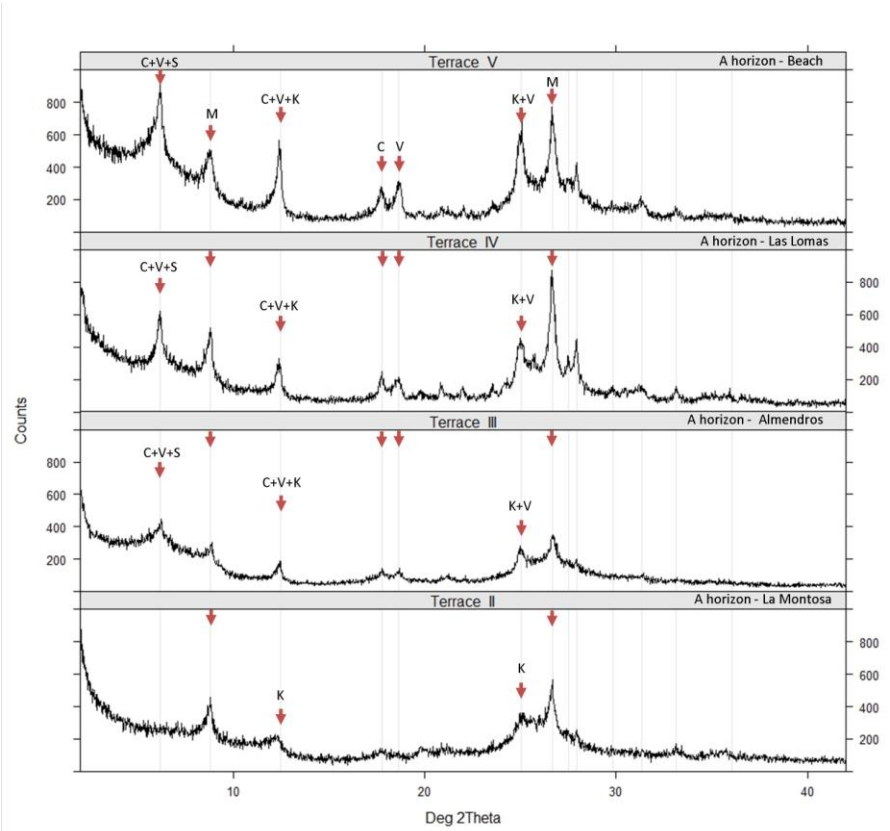

Figure 5. XRD patterns for surface horizons of selected profiles indicating first and second order peaks for: S, smectite; C, chlorite; V, vermiculite; M, muscovite; K, kaolinite

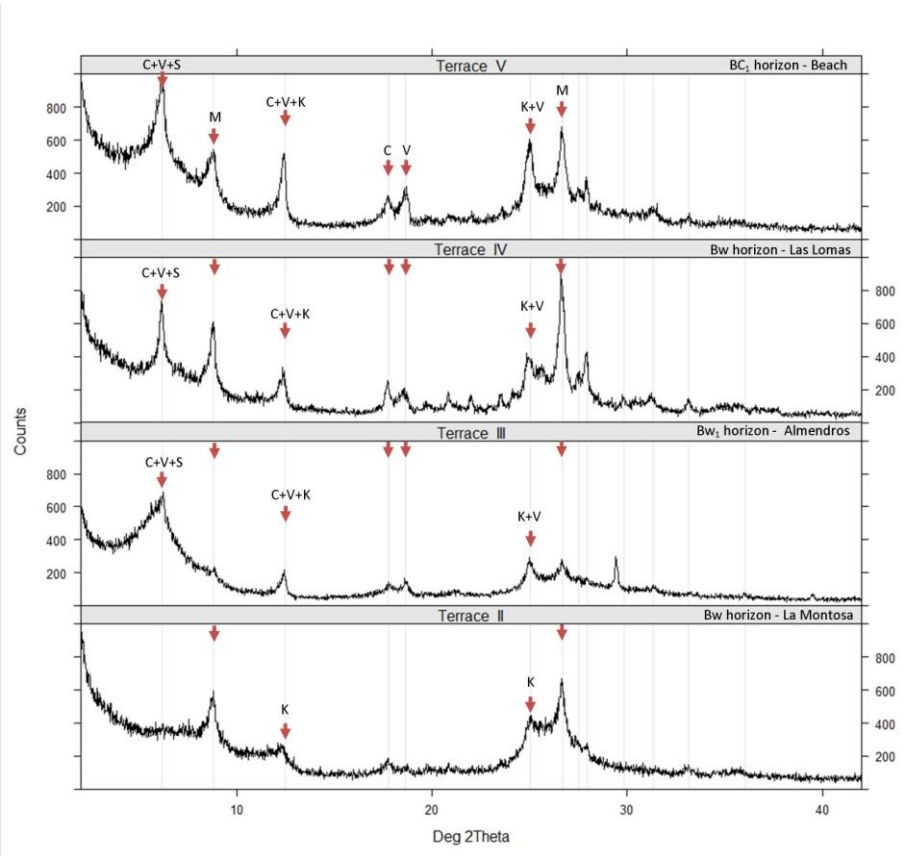

Figure 6. XRD patterns for subsurface of selected profiles (T_V, Beach; T_{IV}, Las Lomas; T_{III}, Los Almendros and T_{II}, La Montosa) indicating first and second order peaks for; S, smectites; C, chlorite; V, vermiculites; M, muscovite; K, kaolinites;

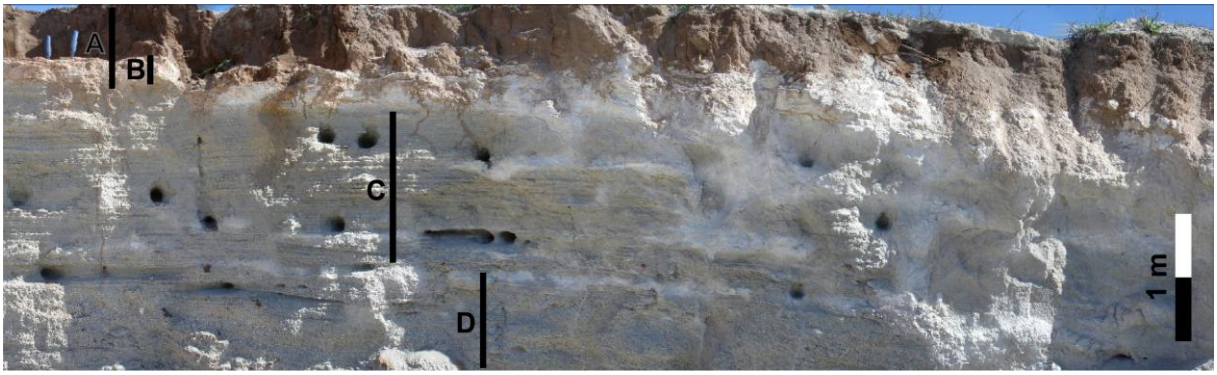

Figure 7. SSE-NNW section of stratigraphic profile near Maitencillo site. A: soil profile. B: calcrete; C: fine sandstone strata with intercalation of siliciclastic and biogenic sand layers of about 1 cm width, with low angle planar lamination; D: strata with high angle planar lamination dipping east, containing shell fragments (5 to 10 mm) in sandy matrix, cemented.

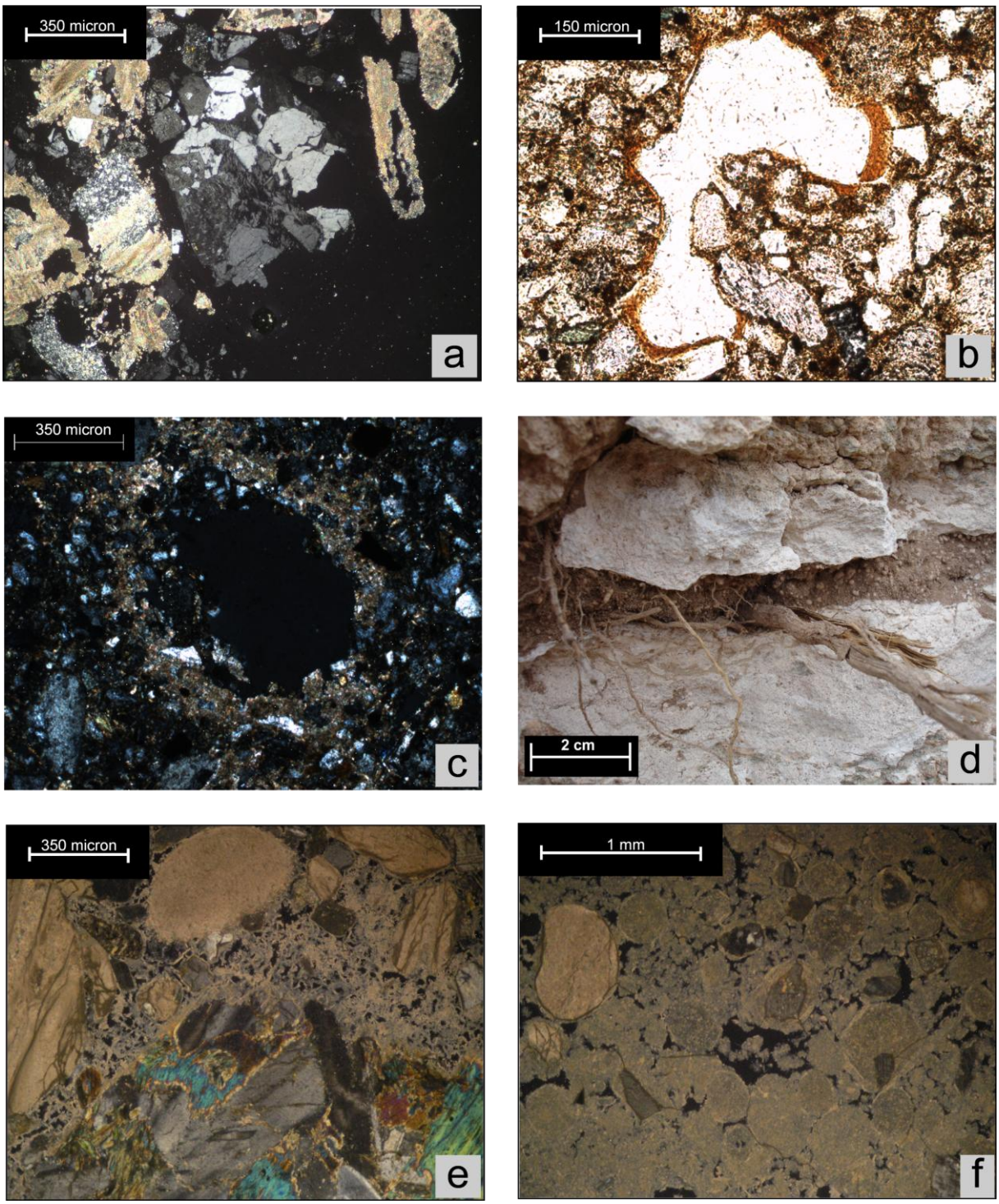

Figure 8. (a) Cross-polarized light (XPL) view of gypsum in massive calcrete in Alamito profile. (b) Clay coating lining a pore in 2Bw horizon of the Las Lomas profile (XPL). (c) Calcium carbonate hypocoating in $2Bt_1$ horizon in the Las Lomas profile (XPL); (d) Fracture in laminar calcrete (pisolithic layer) of the La Montosa profile; (e) Alveolar septal structure in massive calcrete of the El Rincón profile (XPL); (f) Peloids and ooliths in a micritic matrix with vuggy porosity, massive calcrete in the El Rincón profile (XPL).

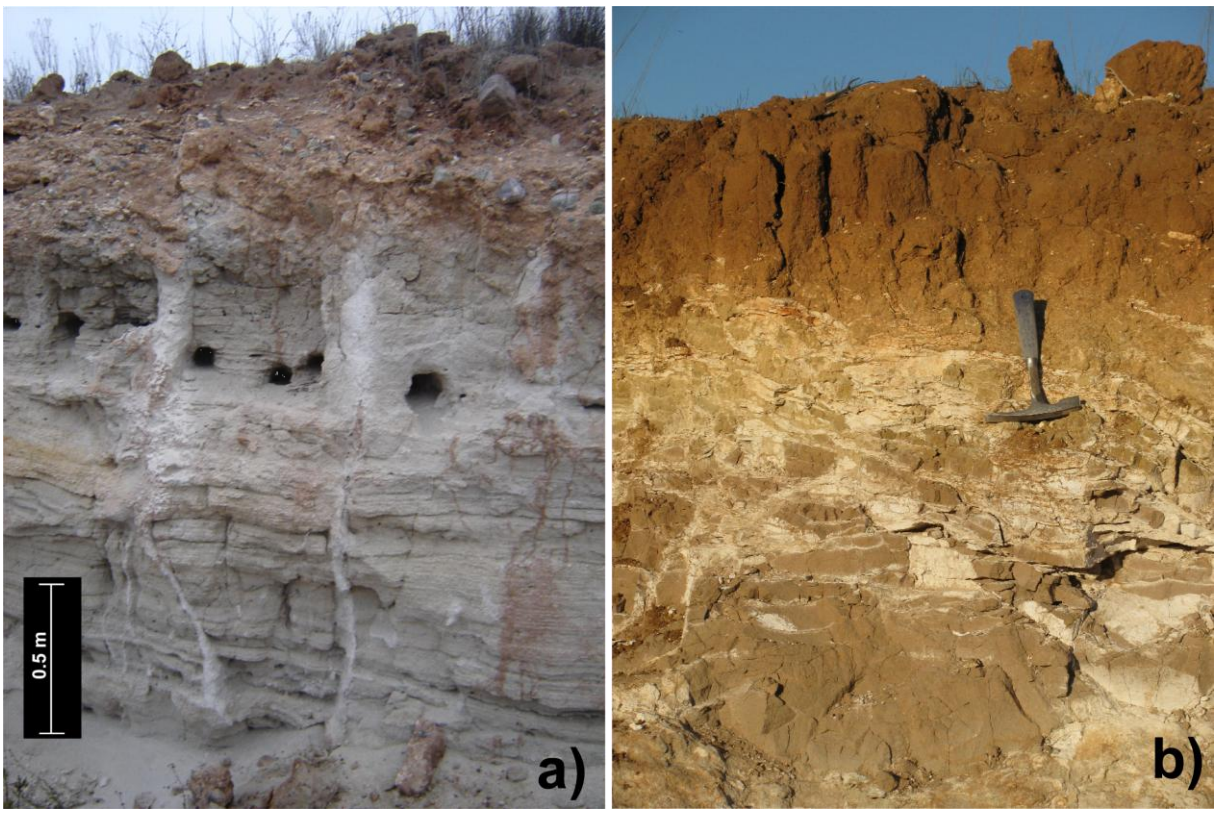

Figure 9. (a) Macroscopic rhizoliths in a mainly siliciclastic sandy matrix, Greditas area at the western limit of the TII terrace. (b) Honeycomb calcrete formation filling fractures of a weakly cemented siliciclastic sandy matrix.

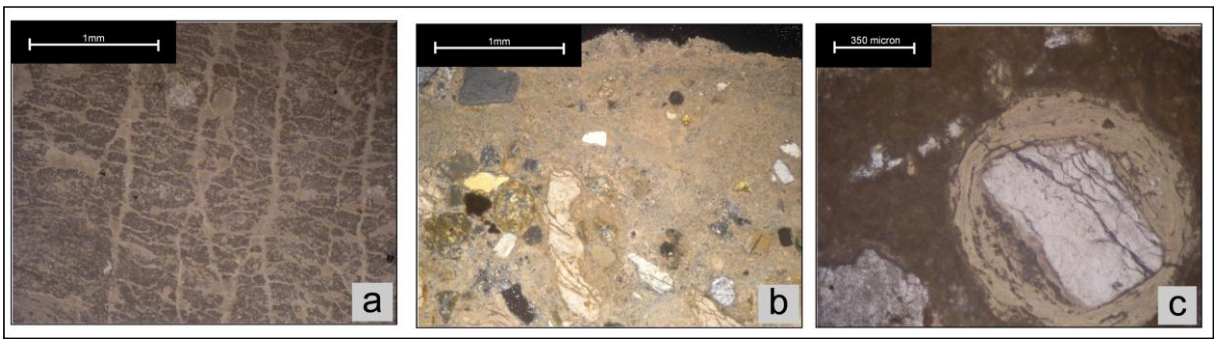

Figure 10. (a) Upper microlaminae of laminar calcrete from El Rincón Profile. Calcium carbonate is principally micritic with undulations and fractures filled with sparitic cement, parallel-polarized light. (b) Upper border of laminar calcrete from Almendros profile. Note the increase in number of siliciclastic and bioclastic grains at the bottom. Channel, vuggy and mouldic porosity can be observed at the bottom, cross polarized light. (c) Oolithic grain with a siliciclastic nucleus in a micritic matrix, laminar calcrete at El Rincón, cross polarized light.

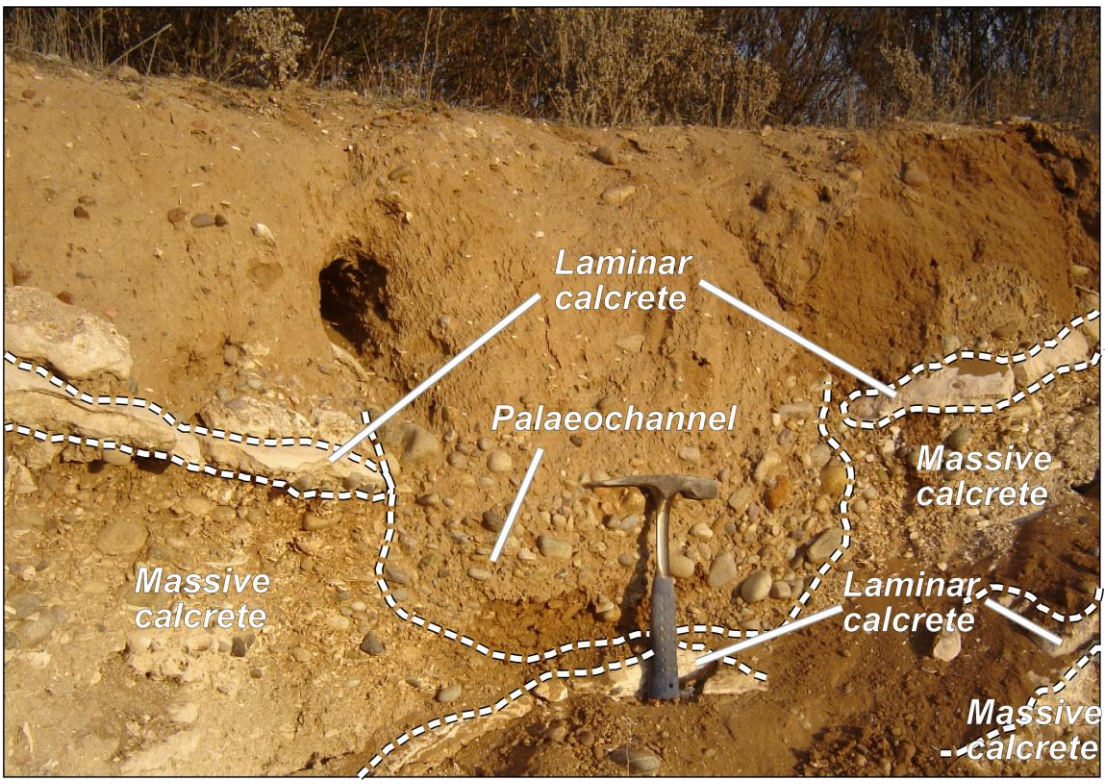

Figure 11. Road-cut profile on TIV terrace (123 ka) showing two superimposed massive and laminar calcrete sequences, the upper of which is eroded by a paleochannel.

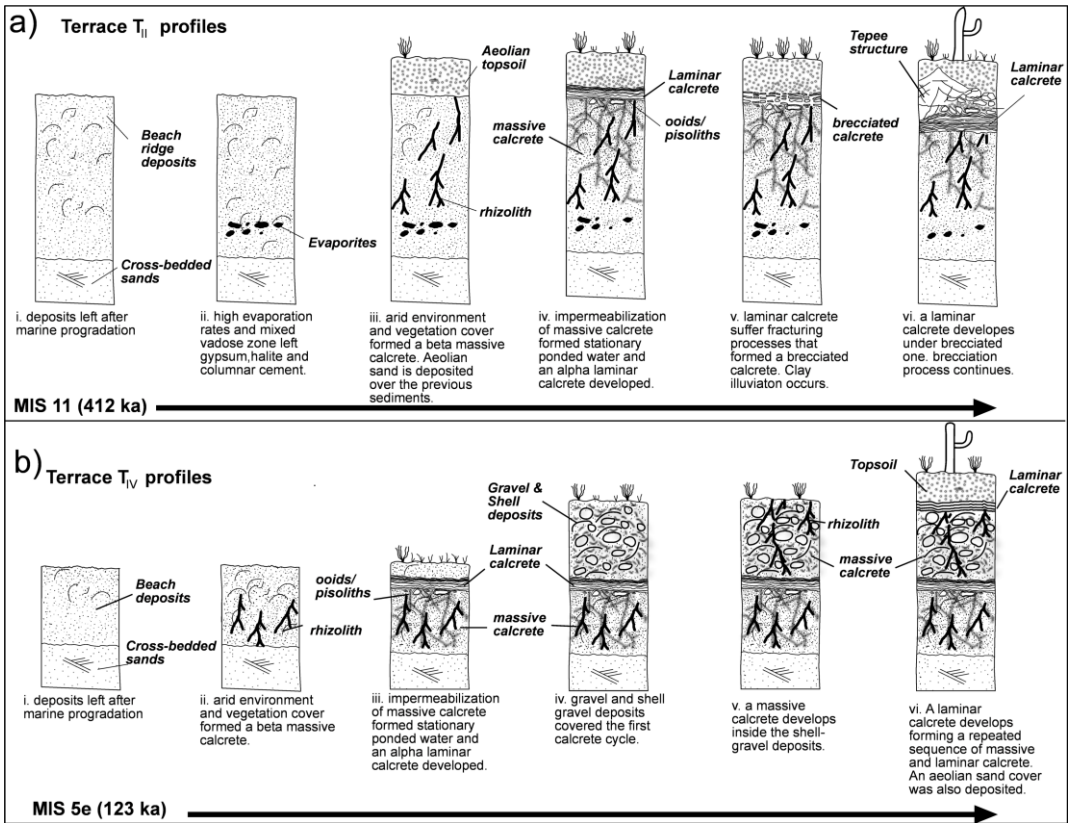

Figure 12. Sequence of events of soil calcrete development at Tongoy corresponding to the TII (a) and TIV (b) terraces.

TABLE CAPTIONS

Table 1. Ages and references of the wave-cut marine terraces in the Tongoy paleobay.

Level	Elevation (masl)	Marine isotopic stage	Age (ka)	Method	References
T_{II}	200	MIS 11	412	U-Th in marine shells	Saillard, 2008
T_{III}	48	MIS 7e	225	^{10}Be in Altos de Talinay	Saillard et al. 2009
T_{IV}	14	MIS 5e	123	U-Th in marine shells	Saillard, 2008
				Geomorphologic correlation with Coquimbo	Ota et al., 1995
T_{V}	9	MIS 1	6	^{10}Be in Altos de Talinay	Saillard et al. 2009
				^{14}C in marine shells	Ota and Paskoff, 1993

Table 2. Soil horizon properties of profiles studied in detail. Abbreviations: Structure: 1 = weak; 2 = moderate; 3 = strong, f = fine; m = medium; c = coarse; vc = very coarse; sbk = subangular blocky; gr = granular; pr = prismatic; cm = columnar; mass = massive. l = laminar; nd = not determined.

Profile	Age	Horizon	Depth	Color (moist)	Structure	B.D.	sand	silt	clay	O.M.	pH	CEC	EC	ESP
	(ka)		(cm)			(kg m^{-3})	(%)	(%)	(%)	(%)	1:2.5	cmol kg^{-1}	dS m^{-1}	(%)
Beach	0.9	A	0-6	2.5Y 5/2	1,f,sbk	1.61	nd	nd	nd	0.36	7.00	7	0.67	0.32
		BC_1	6-15	2.5Y 4/2	1,fm,sbk	1.57	nd	nd	nd	0.24	6.90	4	0.71	0.41
		BC_2	15-41	2.5Y 4/2	1,fm,sbk	1.59	nd	nd	nd	0.76	7.15	8	0.45	0.31
		2C	41-60	5Y 5/2	mass.	1.58	nd	nd	nd	0.17	7.60	9	0.74	0.53
		$3C_1$	60-78	2.5Y 6/2	mass.	1.56	nd	nd	nd	nd	8.80	11	0.81	0.72
		$3C_2$	78-122	5Y 6/2	mass.	nd	nd	nd	nd	nd	8.60	9	0.34	0.03
Las Lomas	123	A	0-4	10YR 4/2	1,f,l	1.61	56.1	32.6	11.3	1.10	7.35	10	0.85	4.06
		Bw	4-12	10YR 4/3	1,m,sbk	1.56	58.0	29.7	12.3	0.28	7.35	11	0.94	5.17
		2Bw	12-32	7.5Y 4/3	3,m,sbk	1.80	49.2	26.5	24.2	1.40	7.40	17	6.15	13.50
		$2Bt_1$	32-49	10YR 5/4	1,c,sbk	1.89	47.0	28.2	24.9	0.13	8.80	16	6.02	24.75
		$2Bt_2$	49-70	10YR 4/3	3,m,sbk	1.88	50.4	21.6	28.0	nd	8.90	21	12.81	20.14
		$2Bt_3$	70-115	10YR 4/3	2,c,pr-3,m,sbk	1.87	48.8	17.7	33.5	0.11	8.92	23	15.38	20.39
		3C	115-124	10YR 5/4	mass.	1.80	78.1	5.2	16.7	nd	9.30	16	6.72	15.26
		4C	124		mass.		92.8	1.0	6.2	nd	9.45	9	1.02	12.24
		5C	124-130	2.5Y 5/3	mass.	nd	91.7	4.0	4.2	nd	9.20	8	4.77	11.82
El Rincón	123	A	0-4	7.5YR 4/4	mass.									
		Bw	4-42	7.5YR 4/4	1,fm,sbk	1.75	86.1	11.7	2.2	1.12	7.20	11.4	0.71	2.63
		C	42-70		mass.	1.75	89.1	9.7	1.2	0.77	7.80	9.14	0.47	2.40
		$2Bkm_1$	~30-~70	7.5YR 8/4		nd	82.0	10.7	7.3	0.38	8.30	10.5	0.64	3.71
Almendros	225	A	0-18	10YR 4/3	2,fm,sbk	1.63	90.0	6.7	3.2	0.56	7.80	9.24	0.53	1.73
		Bw_1	18-54	10YR 6/4	1,fm,sbk	1.75	89.4	5.3	5.3	0.27	8.18	7.45	0.35	1.88
		Bw_2	54-70	10YR 6/4	1,m,sbk	1.76	91.0	3.7	5.3	0.24	8.10	4.61	0.41	4.34
		2Bkm	70-81	10YR 7/3		nd	nd	nd	nd	0.72	8.20	8.08	0.66	4.33
Alamito	350	A	0-1	7.5YR 3/2	mass.	1.49	nd	nd	nd	1.35	7.5	12.00	0.51	6.25
		Bw	1-5	7.5YR 4/4	3,m,sbk	1.61	75.2	15.5	9.3	1.14	8.0	12.00	0.63	7.25
		Bw/Bkm	5-23	7.5YR 3/4	2,mc,sbk	1.56	81.1	11.6	7.3	nd	8.9	15.80	14.85	13.23
		$2Bkm_1$	23-33	7.5YR 7/4	mass.	1.78	76.1	14.2	9.7	nd	8.9	10.20	0.81	1.55
		$2Ckm_1$	33-58	10YR 8/2	mass.	1.62	74.1	17.6	8.3	nd	8.9	9.30	0.32	1.22
		$2Ck_1$	58-70	2.5Y 6/2	mass.	1.54	85.4	9.4	5.2	nd	9.1	8.10	0.44	1.54
La Montosa	370	A	0-5	7.5YR 3/4	3,f,gr	1.68	79.8	8.9	11.3	1.98	7.0	14.40	0.62	4.88
		Bw	5-23	7.5YR 3/4	3,m,sbk	1.71	78.5	9.1	12.4	0.90	7.0	14.70	0.61	6.42
		Bw/Bkm	23-36	7.5YR 3/4	2-3,m,sbk	1.58	78.0	9.6	12.5	1.10	8.0	16.90	17.20	16.85
		2Bkm	36-56	7.5YR 8/3	mass.	nd	nd	nd	nd	nd	9.0	14.80	7.96	4.60
		$2Ck_1$	56-77	2.5Y 5/3	mass.	1.98	78.5	12.2	9.3	nd	8.4	11.40	5.20	11.65
		$2Ck_2$	77-102	5Y 6/2	mass.	2.15	70.2	16.5	13.3	nd	9.0	4.30	11.70	90.41
		2Ckm	102-103	2.5Y 8/2	mass.	1.90	69.6	16.1	14.3	nd	8.9	7.80	83.70	93.66
		$2Ck_3$	103-136	5Y 6/2	mass.	1.71	73.6	16.1	10.3	nd	9.0	8.96	29.80	83.84
Maitencillo	390	A	0-4	7.5YR 3/270	3,f,gr	1.50	86.3	6.5	7.3	1.00	7.3	5.27	62.10	91.22
		Bw	4-12	7.5YR 4/6	2,fm,sbk	1.61	85.2	5.5	9.3	0.90	7.0	8.32	12.80	86.94
		Bt_1	12-26	5YR 4/4	3,c,cm	1.78	66.9	11.9	21.1	0.59	6.4	7.66	20.60	93.12
		Bt_2	26-47	5YR 4/4	2,c,sbk	1.82	63.9	9.5	26.6	0.68	7.0	10.52	61.00	90.83
		Bt_2/Bkm	47-58	7.5YR 8/2	2,fm,sbk	1.87	57.4	8.6	34.0	0.49	8.1	11.15	48.50	93.72
		2Bkm	58-67	10YR 7/3	mass.	nd	nd	nd	nd	nd	8.2	7.64	43.80	94.04
		$2Ck_1$	67-82	2.5Y 8/2	mass.	1.82	58.6	22.0	19.3	nd	8.5	4.30	18.30	96.37
		$2Ck_2$	82-106	2.5Y 6/4	mass.	1.88	83.6	5.1	11.4	nd	8.5	3.93	8.20	96.58
		$2Ck_3$	106-123	2.5Y 8/2	mass.	1.77	68.3	16.2	15.4	nd	8.2	5.98	4.88	95.51
		$2Ck_4$	123-173	5Y 7/2	mass.	1.83	87.7	5.4	6.9	nd	9.1	6.02	20.60	94.13

Table 3. Total chemistry of selected laminae from laminar calcretes of three soil profiles from Tongoy. (LOI: Loss on ignition).

Sample	SiO_2	Al_2O_3	TiO_2	Fe_2O_3	CaO	MgO	MnO	Na_2O	K_2O	P_2O_5	LOI	SUM
La Montosa 1	7.32	1.9	0.36	2.35	48.84	1.01	0.05	0.4	0.39	0.19	36.75	99.56
La Montosa 2	13.61	1.42	0.29	1.85	45.3	0.88	0.02	0.37	0.24	0.09	35.54	99.61
La Montosa 3	11.36	3.01	0.46	3.11	42.85	1.04	0.04	0.41	0.35	0.09	36.79	99.51
Almendros 1	1.76	0.43	0.32	2.39	50.5	0.5	0.03	0.3	0.2	0.15	43.11	99.69
El Rincon 1	3.82	1.37	0.6	2.21	53	1.14	0.04	0.39	0.3	0.25	36.5	99.62
El Rincon 2	1	0.01	0.08	0.33	54.31	1.73	0.01	0.3	0.02	0.1	41.72	99.61
El Rincon 3	0.01	0.01	0.17	0.53	54.91	0.91	0.01	0.3	0.02	0.12	42.55	99.54